Energy 248 (2022) 123601

Contents lists available at ScienceDirect

Energy

journal homepage: www.elsevier.com/locate/energy

Distinguish between the economic optimal and lowest distribution temperatures for heat-prosumer-based district heating systems with short-term thermal energy storage

Haoran Li [a, *], Juan Hou [a], Tianzhen Hong [b], Natasa Nord [a]

[a] Department of Energy and Process Technology, Norwegian University of Science and Technology, Kolbjørn Hejes vei 1 B, Trondheim, 7491, Norway
[b] Building Technology and Urban Systems Division, Lawrence Berkeley National Laboratory, 1 Cyclotron Road, Berkeley, CA, 94720, USA

ARTICLE INFO

Article history:
Received 28 October 2021
Received in revised form
18 February 2022
Accepted 25 February 2022
Available online 28 February 2022

Keywords:
4th generation district heating
Low distribution temperature
Economic optimization
Thermal energy storage
Heating price
Peak load

ABSTRACT

Decreasing distribution temperature is the key driving force for energy-efficient and economic-competitive district heating (DH) systems, powering the transition from the 1st generation high-temperature steam-based DH systems to the 4th generation low-temperature water-based DH systems. However, for heat prosumers integrated with thermal energy storages (TESs), the decreasing distribution temperature may lower the peak load shaving capability of TESs and raise the peak-load-related heating costs, due to decreased charging temperature. This study, therefore, aimed to investigate the overall impacts of distribution temperature and to identify the economic optimal distribution temperature for heat-prosumer-based DH systems integrated with short-term TES. Firstly, an economic optimization problem was developed. Afterwards, distribution temperatures were optimized within the feasible regions of individual scenarios, including three benchmark scenarios representing the 2nd, 3rd, and 4th generation DH and an improved scenario featured high feasibility in distribution temperature. A campus DH system in Norway was used as the case study. Results revealed that the improved scenario's economic optimal distribution temperature was significantly distinct from the 4th generation DH scenario's lowest distribution temperature, both in terms of distribution range and annual average level. Finally, broad conclusions were reached by discussing the impacts of crucial factors on economic optimal distribution temperatures.

1. Introduction

In the European Union (EU), buildings are responsible for approximately 40% of total energy use and 36% of greenhouse gas emissions [1]. Space heating (SH) and domestic hot water (DHW) systems, as essential parts of building energy systems, play an important role in buildings' energy use. For example, in the residential sector of the EU countries, about 80% of the energy use is for SH and DHW [2,3]. District heating (DH) systems make it possible to satisfy buildings' heat demand in an environment-friendly and energy-efficient way [4]. Moreover, compared with alternative heating technologies, DH is competitive, especially for urban areas with concentrated heat demand. Nowadays, about 80,000 DH systems are working successfully worldwide, thereof about 6000 DH systems are in Europe [5]. Moreover, for some countries, the national heat market share of DH can reach 60% [5–7]. To maintain competitiveness and guarantee continuous success, the current 2nd and 3rd generation DH systems are transforming into the 4th generation DH (4GDH) systems [8–10]. The salient feature of this transformation is the decreasing distribution temperature, including the supply and return temperatures. This temperature reduction will improve the energy efficiency of the future DH systems and thus improve their economic performance [4,11]. According to research on typical Swedish DH systems, the expected average cost saving from this temperature reduction is 0.15 €/(MWh·°C) [12]. Furthermore, with a possible cost-saving of 0.65 €/(MWh·°C), the economic benefits will be more significant for renewable-based DH systems [13].

Due to the above benefits, a large and growing body of studies has investigated the future low-temperature DH systems, i.e., 4GDH systems. Among these studies, some focused on the heat demand side, i.e., heating systems in buildings. The low supply temperature

* Corresponding author.
E-mail address: haoranli@ntnu.no (H. Li).

https://doi.org/10.1016/j.energy.2022.123601

Nomenclature

4GDH	4th generation DH
DC	Data centre
DH	District heating
DHW	Domestic hot water
DHS	Distributed heat source
EDC	Energy demand component
FDC	Flow demand component
FXC	Fixed component
HE	Heat exchanger
LDC	Load demand component
MS	Main substation
R2R	Extraction from the return line and feed into the return line
RF	Renewable fraction
SH	Space heating
TES	Thermal energy storage
WCC	Weather compensation control
WTTES	Water tank thermal energy storage

of future DH systems may be not compatible with heating systems in existing buildings that have been designed with higher temperatures. This temperature incompatibility may cause problems, such as unexpected low indoor air temperature for the SH system and hygiene issues for the DHW system. Recent studies have proposed technological and economically feasible measures to solve these problems. Regarding the SH system, the measures may be improving system control [12,14–16], renovating building envelopes [17,18], and replacing radiators [12,17,19–21] and thermal valves [22]. Regarding the DHW system, the measures may be installing supplementary heating devices, e.g., direct electric heaters or micro heat pumps [23].

Moreover, some studies focused on the heat supply side, i.e., heating sources, thermal energy storages (TESs), and distribution networks. A case study in North Japan with the cold winter season showed that the primary energy use of combined heat and power plants can be saved by 7% after the transition to the low-temperature DH system [24]. A case study located in North Estonia also with the cold winter season showed that the saving can be up to 47% if replacing the high-temperature fossil-fuel-based plants (gas-fired boilers) with low-temperature renewable-based plants (large-scale heat pumps using seawater as heat source) [25]. Due to the transition to the low-temperature DH system, the distribution heat loss will be reduced as well. For a DH system consisting of low energy and passive house buildings in Norway, the heat loss reduction would be 25% for one year [26]. For another DH system in Norway, one-third of yearly heat loss reduction could be achieved [27]. Moreover, 34% of annual heat loss could be reduced for a hypothetical DH system that was designed to supply heat for 30 detached residential houses in Denmark [28]. The reduced heat loss can improve the energy efficiency of DH systems remarkably, because of the large share of the distribution heat loss, which can be up to 35% [29] of the delivered heat.

These previous studies have demonstrated the benefits of the low-temperature DH system and proposed technical solutions to support the transition to the future low-temperature DH systems. However, these studies are subject to the following limitations. Firstly, regarding the research method, previous studies tended to separate the research problem into two subproblems: the heat-demand-side problem and the heat-supply-side problem. They mostly conducted isolated research on either side and ignored the coupling between the two sides. For example, studies [24–28] evaluated the benefits on the supply side brought by the reduced distribution temperature, however, they ignored the temperature compatibility issues on the demand side. Secondly, regarding the scope of research, previous studies mainly focused on DH systems with central heat sources yet gave less attention to heat-prosumer-based DH systems with distributed heat sources (DHSs). In the future, heat prosumers will become essential participants in DH systems because of the increasing integration of renewable energies, e.g., waste heat from refrigeration systems and industrial processes or utilization of solar thermal energy [30–33]. More research is needed to gain a deeper understanding of how distribution temperature impacts the performance of heat-prosumer-based DH systems.

Last but most importantly, regarding the technology roadmap, previous studies have been dedicated to enhancing DH systems' economic performance by improving their energy efficiency, which can be achieved by lowering the distribution temperature. However, DH systems' economic performance depends not only on energy efficiency, but also on peak load. Peak load can have a considerable amount of influence over DH systems' investments as well as operating costs. For the investment, peak load determines the capacities of heating plants and distribution networks. Higher peak loads always mean higher capacities of heat generation and distribution, and hence higher investment costs for DH systems. For the operation cost, peak load is generally covered by peak load heating plants which always have higher operating costs than baseload heating plants. The presence and share of the peak-load-related components in heating pricing models may be used as indicators to evaluate peak load's economic impacts. A survey of 237 heating pricing models in Sweden found that 87% of the investigated heating pricing models contained a peak-load-related component, i.e., Load Demand Component (LDC) [34]. Furthermore, the peak-load-related component accounted for a significant portion of the total heating cost, with a sharing of 28% on average [34]. These indications revealed that in heating pricing models, the peak-load-related component is the second most significant component after the energy-use-related component, i.e., the Energy Demand Component (EDC). Introducing TESs is one of the most used solutions to shave the peak load of DH systems [35–38]. However, the decreasing distribution temperature, which is driving the development of DH systems by improving their energy efficiency, may reduce the peak load shaving effect of TESs, resulting in higher peak-load-related heating costs for heat users. Since the charging temperature of TESs drops with the decreasing distribution temperature of DH systems, which further reduces the storage temperature as well as the storage capacity of TESs. The peak load shaving effect of TESs, which is positively correlated to the storage temperature and the storage capacity, would be impaired. Therefore, as presented in Fig. 1, there is a trade-off between the energy efficiency of DH systems and the peak load shaving effect of TESs. Given the significant economic importance of DH systems' energy efficiency and peak load, further research is needed to understand how distribution temperature influences these two factors, and hence the overall economic performance of DH systems.

To overcome the above limitations and fill the knowledge gap, this study, therefore, aimed to economically optimize the distribution temperature for heat-prosumer-based DH systems integrated with short-term TES in a dynamic heating market, considering the coupling between the supply and demand sides. To achieve this goal, a dynamic optimization framework to optimize the distribution temperature was proposed. In the optimization framework, both economic boundaries and system models were generalized to make the research method and findings more applicable. Regarding the economic boundaries, a generalized

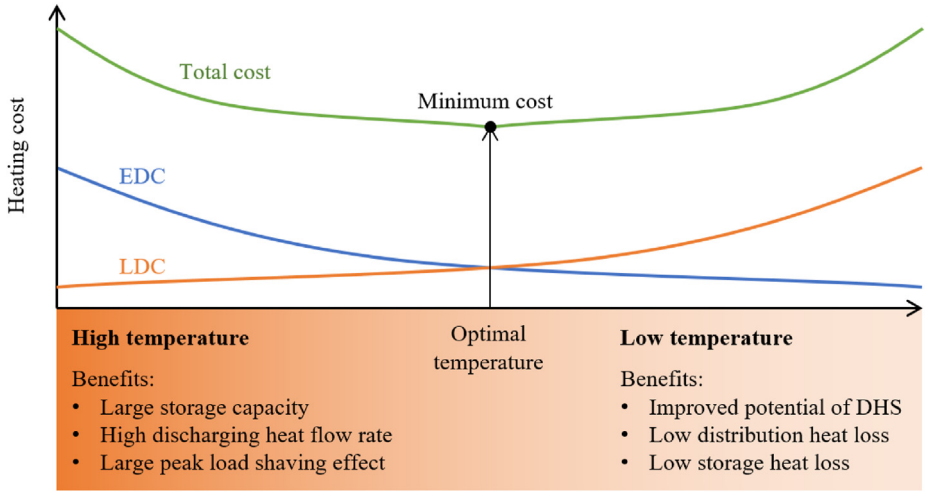

Fig. 1. Benefits for high and low distribution temperature.

heating pricing model represented the pricing mechanism in the current Scandinavian heating market was used. Regarding the system model, it was developed based on a typical heat-prosumer-based DH system, which integrated a renewable-based DHS and a short-term TES. To evaluate the performance of the proposed optimization framework as well as to study the impacts of the distribution temperature, scenarios representing various levels of distribution temperatures were designed. The proposed method was tested on a campus DH system in Norway, which was a heat-prosumer-based DH system with a DHS that recovered the waste heat of a university data centre (DC). The studied system was monitored by the university energy management platform, and detailed operation data were available to facilitate the study.

The contributions of this study lie in the following aspects. Firstly, the developed optimization framework was able to reduce heat prosumers' heating costs under dynamic heating prices, while considering the coupling between the supply and demand sides of DH systems. Secondly, the impacts of distribution temperature on the energy and economic performance of heat-prosumer-based DH systems with TES were investigated. The findings made a pioneering effort to distinguish between the economic optimal distribution temperature (which considers both the energy efficiency and peak load) and the lowest distribution temperature (which is purely based on the energy efficiency). Finally, data collected from the university's energy management platform were used in the case study. The results validated the effectiveness of the proposed research method.

The remaining of the article is organized as follows: Section 2 introduces the typical heat-prosumer-based DH system and explains the formulated dynamic optimization problem. Section 3 presents the background of the case study, research scenarios, and simulation settings. Section 4 explains the research results, and Section 5 and Section 6 discuss and conclude this study.

2. Method

This section firstly introduces a typical heat-prosumer-based DH system with a DHS and a TES. Afterwards, an economic optimization problem to optimize the distribution temperature and minimize the heating cost is introduced. Finally, the method to deal with the coupling between the supply and demand sides is explained.

2.1. Typical heat-prosumer-based DH system with a DHS and a TES

Configurations of heat-prosumer-based DH systems may vary from case to case. To generalize the research method, however, a typical heat-prosumer-based DH system was developed. This typical system, which included buildings, a main substation (MS), a DHS, and a short-term TES, is illustrated in Fig. 2.

In this typical system, the buildings could be one single or a cluster of commercial, residential, or industrial buildings. The DHS was a renewable-based and low-temperature heat source that may recover waste heat from a DC or utilize solar thermal energy. There are three commonly used connection modes for feeding heat from a DHS into a DH grid: 1) the from return to supply (R2S) mode extracts water from the return line, heats it to the required temperature, and then feeds it into the supply line, 2) the from return to return (R2R) mode extracts water from the return line, heats it to any temperature higher than the extracted water, and then feeds it into the return line, and 3) the from supply to supply (S2S) mode extracts water from the supply line, heats it to any temperature higher than the extracted water, and then feeds it into the supply line [4,39]. Among these connection modes, the R2R connection mode has the lowest extracted water temperature as well as the potential for a low temperature rise for the heating process. Due to these advantages, R2R mode is preferred for low-temperature DHSs like solar thermal plants and heat pumps [33,39,40]. Therefore, the R2R mode was selected in this study. Moreover, the heat prosumer's regional DH system was connected to the city central DH system by an MS, in which two heat exchangers (HEs) were installed: HE1 and HE2. The HE1 was connected to the TES for charging purposes, thus it was called the charging HE; HE2 was connected to the main pipelines of the prosumer's regional DH system to boost the supply temperature to the required level, thus it was called the boosting HE.

The TES was a short-term one with two basic functions: mismatch relieving and peak load shaving. Firstly, it solved the mismatch problem. During the warm periods, the DHS's non-dispatchable heat generation may be counter to the buildings' heat demand, which means surplus heat supply from the DHS may exist when the buildings' heat demand is lower. The surplus heat supply would be fed into the central DH system through the MS, however, heat prosumers gain no economic benefits from this heat supply, because the current widely used heating price models have not yet supported the reverse heat supply from heat users to the

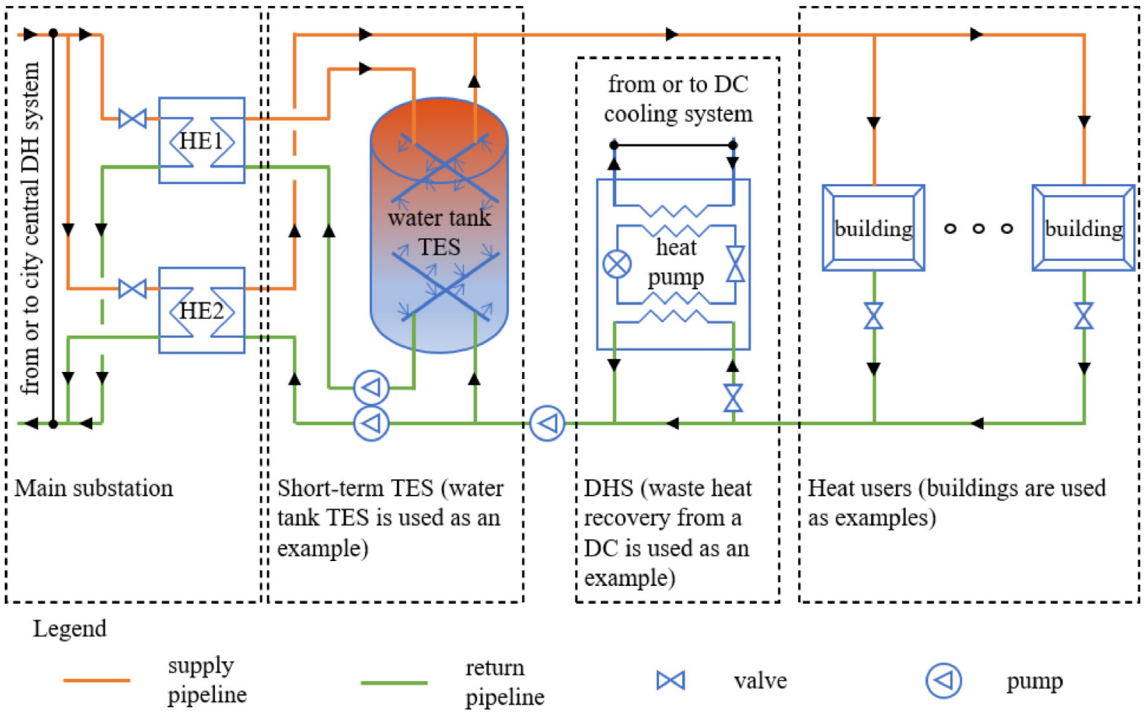

Fig. 2. A typical heat-prosumer-based DH system with a DHS and a TES.

central DH system [34]. TES is a long-proven technology to solve the mismatch problem, it can store the surplus heat for later use [41–45]. Secondly, the TES shaved the peak load. During the cold periods, DH systems may have peak loads that are significantly higher than the normal level. Even these peak loads may last only for a few hours, they can have a considerable impact on the annual heating cost. Since DH companies usually charge the heating bill considering heat customers' peak loads, and the heating cost related to the peak load may account for up to 50% of the total heating cost [34]. TESs have been widely used for peak load shaving in DH systems, they can shift part of the heat supply from peak hours to non-peak hours [35–37].

2.2. Formulation of the temperature economic optimization problem

This section explains the proposed optimization framework to optimize the distribution temperature of heat-prosumer-based DH systems, while minimizing the heat prosumer's heating cost. Firstly, a generalized heating price model was developed based on a literature review on the current heating price models in the Scandinavian heating market. Afterwards, under this generalized heating price model, a dynamic optimization framework was proposed based on the typical heat-prosumer-based DH system developed in Section 2.1.

Current widely used heating price models in the Scandinavian heating market may contain four components: EDC, LDC, flow demand component (FDC), and fixed component (FXC) [34]. These four components are paid by heat users to DH companies. The EDC is charged based on end users' heat use. It aims to cover the production cost that mainly refers to the fuel cost. The LDC is usually charged according to the end user's peak load. It reflexes DH companies' investment cost for new facilities, depreciation of existing facilities, operating cost to maintain a certain level of heat generation capacity, etc. Generally, the FXC is also charged according to end users' peak load. It is the connection fee for heat users to stay in the heating grid. Circulation cost is presented by the FDC. The FDC is charged based on the volume of the circulating heat carrier, i.e., hot water. It aims to cover the circulating electricity cost for heat delivery. Moreover, FDC stimulates to lower the return temperature.

Among these four components, LDC and EDC are crucial, regarding both their presence and share in a heating price model. As illustrated by Fig. 3, a survey on heating price models in Sweden shows that all the heating price models have the EDC and about 87% of them have the LDC. These two parts together account for 96% of the total heating cost on average. In contrast, just about half of the heating price models have FXC and FDC, and the average share of the two components is less than 2%. Therefore, the heating price models can be simplified and approximated by erasing the insignificant components, i.e., FXC and FDC, while including the crucial components, i.e., LDC and EDC. Consequently, to optimize the distribution temperature and minimize the heating cost of a heat-prosumer-based DH system, a multi-objective economic optimization problem was formulated by Equations (1), (2), (3), (4) and (5). In addition, the concept of this optimization framework is illustrated in Fig. 4 and detailed descriptions of the modelling work can be found in the study [46].

Minimize:

$$\int_{t_0}^{t_f} EP(t) \cdot \dot{Q}(t)dt + LP \cdot \dot{Q}_{pea} \tag{1}$$

subject to:

$$\dot{Q}(t) \le \dot{Q}_{pea} \tag{2}$$

$$F(t, \boldsymbol{z}(t)) = 0 \tag{3}$$

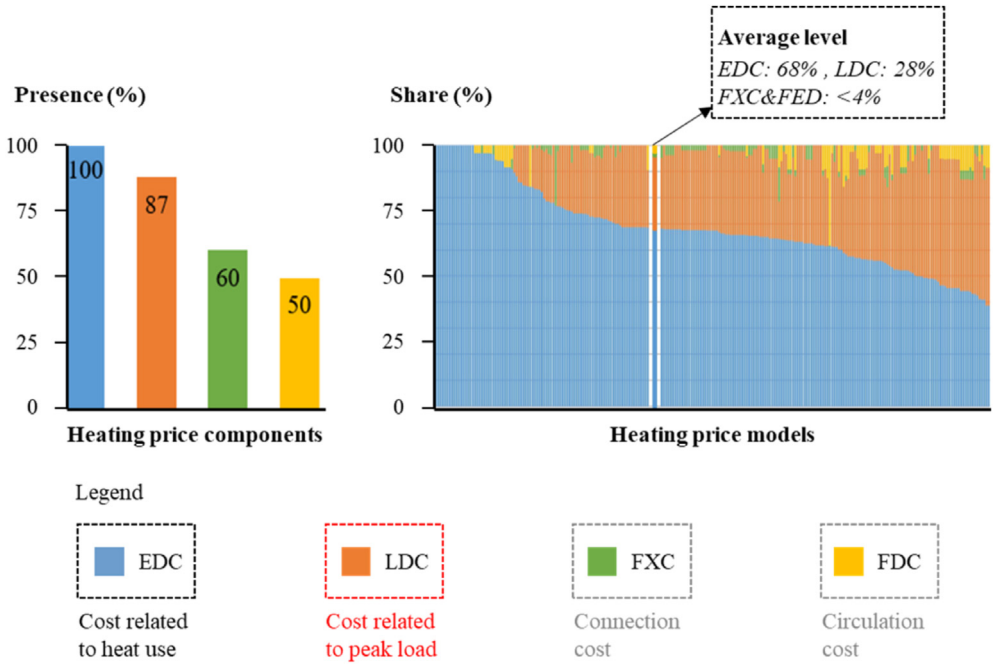

Fig. 3. The presence and share of price components for investigated heating price models [34].

$$F_0(t_0, \boldsymbol{z}(t_0)) = 0 \tag{4}$$

$$z_L \leq \boldsymbol{z}(t) \leq z_U \tag{5}$$

where the first and second term of Equation (1) is the EDC and LDC heating cost, respectively. $EP(t)$ and LP is the heating price for the EDC and LDC, respectively. $\dot{Q}(t)$ is the heat supply rate from the central DH system to the heat prosumer and $\dot{Q}_{pea}$ is the corresponding peak load. Due to the installation of smart meters and the trend of digitalization, an increasing number of DH companies are starting to utilize hourly measured heat use to define the peak load in their heating price models. Therefore, this study used the maximum hourly heat use in one year to define the peak load. Equation (3) defines the dynamics of the heat-prosumer-based DH system proposed in Section 2.1, and Equation (4) specifies the initial conditions of this system. $\boldsymbol{z} \in \mathbb{R}^{n_z}$ are the time-dependent variables, including the manipulated variables $\boldsymbol{u} \in \mathbb{R}^{n_u}$, the differential variables $\boldsymbol{x} \in \mathbb{R}^{n_x}$, and the algebraic variables $\boldsymbol{y} \in \mathbb{R}^{n_y}$. $z_L \in [-\infty, \infty]^{n_z}$ and $z_U \in [-\infty, \infty]^{n_z}$ represent the lower bounds and upper bounds, respectively.

In the proposed dynamic optimization problem, there were five manipulated variables $\boldsymbol{u}$, representing the supply side management as well as the demand side management. For the supply side management that aimed to optimize the distribution temperature, the manipulated variables were the supply temperature and the water flow rate of the MS, i.e., $T_{HE1,sup}$, $T_{HE2,sup}$, $\dot{m}_{HE1}$, and $\dot{m}_{HE2}$. For the demand side management that responded to the supply side management, the manipulated variable was the water flow rate of the buildings, i.e., $\dot{m}_{Bui}$. All these manipulated variables are depicted in Fig. 4.

The optimization problem was solved on the optimization platform JModelica. The formulated optimization problem was infinite-dimensional and was discretized into finite-dimensional nonlinear programming (NLP) problem by a direct collocation method [48]. Afterwards, the discretized finite-dimensional NLP problem was solved using the NLP solver, Interior Point OPTimizer (IPOPT), as the following steps. Firstly, the inequality constraints in the NLP problem were eliminated using the interior-point method [49]. Then a local optimum for the NLP was achieved by solving the first order Karush-Kuhn-Tucker condition, using iterative techniques through Newton's method.

2.3. Coupling between the supply side and the demand side

As introduced in Section 1, the coupling between the supply and demand sides should be considered. In this study, it was considered in the following two aspects. Firstly, the supply temperature of the supply side should be high enough to avoid any problem on the demand side due to insufficient heating capacity. Secondly, the maximum temperature difference between the supply and return water of the supply side should be restricted by the thermal characteristics of the heating systems on the demand side.

The above couplings were treated as bounds in the optimization problem. For the supply temperature, Equation (6) gives the lower bound, which represents the temperature requirement for both the SH system and the DHW system. Regarding the SH system, the lower bound, $T_{sup,SH,L}$, should maintain a comfortable indoor air temperature and it is related to the outdoor temperature and the performance of the radiator as presented in Equation (7) [50]. Regarding the DHW system, the lower bound, $T_{sup,\ DHW,L}$, should avoid hygiene problems and the required temperature under different conditions can be obtained from European standard CEN/TR16355 [51].

$$T_{sup,L} = max\left(T_{sup,SH,L}, T_{sup,\ DHW,L}\right) \tag{6}$$

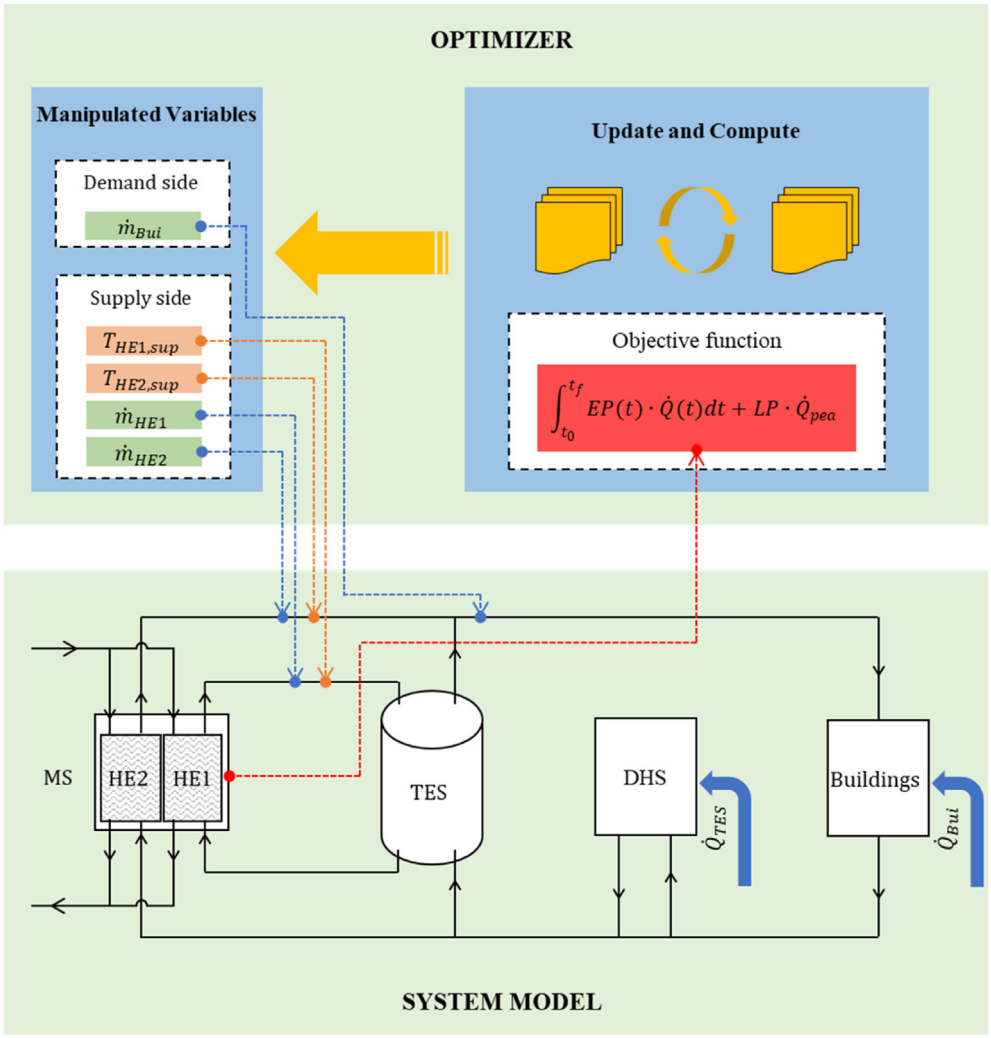

Fig. 4. Schematic diagram of the optimization framework.

$$T_{sup,SH,L} = T_{ia} + 0.5 \cdot \left(T_{sup,SH,des} + T_{ret,SH,des} - 2 \cdot T_{ia}\right) \cdot \left(\frac{T_{ia} - T_{oa}}{T_{ia} - T_{oa,des}}\right)^{1/b} + 0.5 \cdot \left(T_{sup,SH,des} - T_{ret,SH,des}\right) \cdot \left(\frac{T_{ia} - T_{oa}}{T_{ia} - T_{oa,des}}\right) \quad (7)$$

where T_{ia} and T_{oa} are the indoor and the outdoor air temperature, respectively. b is a parameter depending on the characteristic of the radiator. The subscript *des* refers to the design conditions, and the subscript L represents the lower bounds.

For the temperature difference, the upper bound is constrained by the characteristics of the heating system inside buildings, and it is positively correlated with the supply temperature. In this study, it was assumed that the upper bound of the temperature difference could be explored by measured data. This assumption might underestimate the maximum temperature difference of a DH system; however, it guaranteed the temperature difference within its feasible range (defined by the optimization problem) and offered a straightforward way by using measured data. A linear regression model was used to describe the upper bound of the temperature difference, $\Delta T_{dif,U}$, as presented in Equation (8).

$$\Delta T_{dif,U} = a_0 + a_1 \cdot T_{sup} \quad (8)$$

where a_0 and a_1 are parameters.

3. Case study and research scenarios

This section firstly introduces the case study, which is a university campus DH system. Afterwards, research scenarios and simulation settings are explained.

3.1. Background of the case study

The studied DH system is in Trondheim, Norway. As illustrated in Fig. 5, as a heat prosumer, the campus DH system has a DHS that recovers the waste heat from the university DC, meanwhile, it is

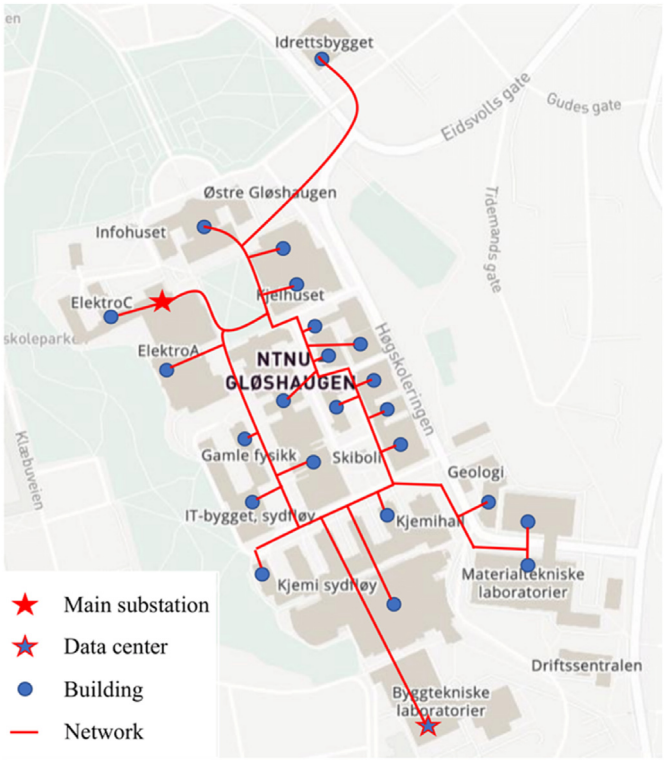

Fig. 5. Campus district heating system.

connected to the city central DH system and get heat supply through the MS. The system supplies heat to 24 university buildings with a total building area of about 300,000 m^2 [52,53]. Fig. 6 presents the measured building heat demand and waste heat recovery from the DC. It is found that the total heat supply of the campus DH system was 32.9 GWh from June 2017 to June 2018, including about 80% coming from the city central DH system and about 20% coming from the DC's waste heat recovery.

The campus DH system demonstrates the potential of heat-prosumer-based DH systems that utilize DCs' waste heat, which reaps significant economic and social benefits. However, the system is facing the following problems. The first problem is the mismatch between the waste heat supply and the building heat demand, which is common for DH systems that utilize non-dispatchable renewable energies. As shown in Fig. 6 (a), the hourly DC waste heat recovery was represented by the green line and were positive values, which would be supplied for the campus DH system. However, there was a mismatch between the DC waste heat supply and the building heat demand. The building heat demand fluctuated between 0 MW and 14 MW for the studied year, while the waste heat recovery was almost a constant heat flow rate of around 1 MW. When the building heat demand was less than 1 MW, not all the DC waste heat recovery could be utilized by the campus DH system, and the unutilized DC waste heat recovery was delivered from the campus DH system to the city central DH system via the MS. This reversed heat flow of the MS was called surplus waste heat and was represented by negative values as shown by the red line in Fig. 6 (a). As shown in Fig. 6 (b), about 1.7 GWh out of 8.7 GWh recovered waste heat became surplus heat supply, accounting for 20% of the total waste heat recovery. The surplus waste heat is supplied to the central DH system through the MS; however, the university does not get any benefit from this heat supply because the local heating price models have not yet supported the reverse heat supply from heat users to the central DH system. The second problem is high peak loads. As shown in Fig. 6 (a), the building heat demand was not equally distributed and there were peak loads. The maximum building heat demand was 14 MW, and it was about four times higher than the annual average level. The heating price model used by the local DH company considers the peak loads, and about 20% of the university's heating cost is linked to the peak load.

Introducing TESs can address the above problems. Moreover, previous research has shown that water tank thermal energy storage (WTTES) is a suitable solution with high energy and economic performance [32]. However, further research is needed to optimize its distribution temperature after introducing the WTTES. As introduced in Section 1, both high and low distribution temperatures can benefit the DH system. A high distribution temperature means a high charging temperature and thus a large storage capacity for WTTES under a certain storage volume. Consequently, a high discharging heat flow rate and a large peak load shaving effect can be achieved by the WTTES. In contrast, a low distribution temperature means a large waste heat recovery potential for the DC. Moreover, the heat loss of both the distribution system and the WTTES can be reduced. Therefore, the resulting economic impacts of the distribution temperature are: 1) increasing the distribution temperature can reduce the LDC heating cost that is related to peak load, and 2) reducing the distribution temperature can save the EDC heating cost that is related to heat use. This study developed a method to optimize the distribution temperature and make a trade-off between these two impacts.

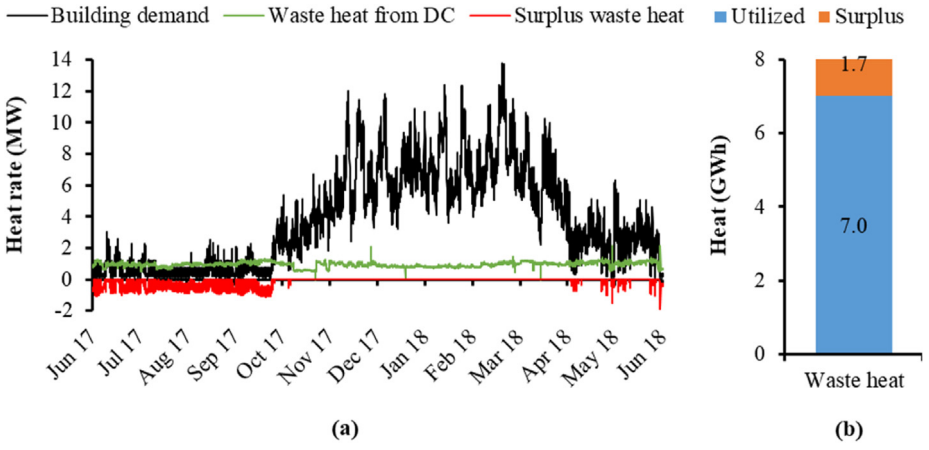

Fig. 6. Heat demand and waste heat supply.

Table 1
Information on the scenarios.

Abbreviation	Feasible region of the supply temperature	Note
Op-Temp	Region Op-Temp in Fig. 7, ranging from 50 °C to 120 °C.	This scenario had the largest feasible region with the highest flexibility in supply temperature. It was an improved scenario that obtained the **Economic Optimal Distribution Temperature**.
H-Temp	Region H-Temp in Fig. 7, ranging from 100 °C to 120 °C.	This scenario had a high supply temperature that represented 2nd generation DH systems. It was a benchmark scenario.
M-Temp	Region M-Temp in Fig. 7, ranging from 80 °C to 100 °C.	This scenario had a medium supply temperature that represented 3rd generation DH systems. It was a benchmark scenario.
L-Temp	Region L-Temp in Fig. 7, ranging from 50 °C to 80 °C.	This scenario had a low supply temperature that represented 4th generation DH systems. It was a benchmark scenario, which obtained the **Lowest Distribution Temperature**.

3.2. Scenarios and simulation settings

To study the economic impacts of distribution temperature on heat-prosumer-based DH systems with TESs, and identify the economic optimal distribution temperature, four research scenarios were designed, i.e., *Op-Temp*, *H-Temp*, *M-Temp*, and *L-Temp*. These scenarios used an identical operation strategy proposed in Section 2, however, applied different levels of distribution temperature. The basic information of these scenarios is presented in Table 1, and the corresponding supply temperatures are illustrated in Fig. 7. The upper bound in Fig. 7 was determined by the supply temperature of the central city DH system, and the lower bound was obtained by Equation (6). As presented in Table 1, Scenarios *H-Temp*, *M-Temp*, and *L-Temp* represented the distribution temperature levels of the 2nd, 3rd, and 4th generation DH systems, respectively. These scenarios were used as benchmarks. In contrast, Scenario *Op-Temp* had the highest flexibility in distribution temperature, and it was an improved scenario compared to the benchmark scenarios. The impacts of distribution temperature on the performance of heat-prosumer-based DH systems would be revealed by comparing the outcomes of the benchmark scenarios. Meanwhile, comparing the outcomes of Scenarios *Op-Temp* and *L-Temp* would highlight the difference between the economic optimal and lowest distribution temperatures.

Key simulation settings are presented in and Table A. 1 and Fig A. 1 in Appendix A. Detailed information on the settings can be found in the paper [46]. The input variables of the buildings' heat demand and the DC's waste heat were obtained from measurement as presented in Fig. 6. This study used Modelica language [54] to build the system model and the JModelica platform [55] to formulate and solve the optimization problem.

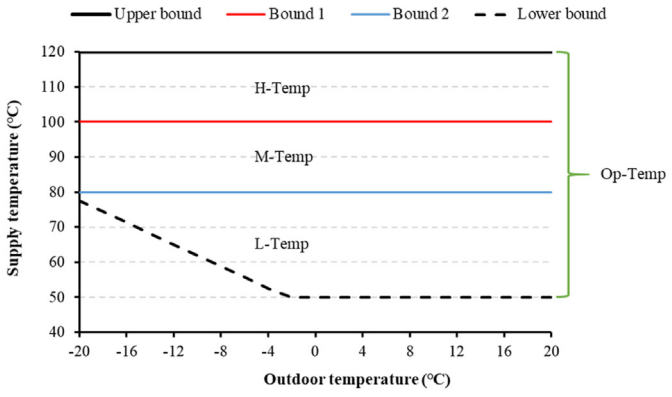

Fig. 7. Feasible region of supply temperature for the four scenarios.

4. Results

This section presents the results. Firstly, the validation results are introduced in Section 4.1. Secondly, the distribution temperatures of the four scenarios are evaluated and compared in Section 4.2. Afterwards, the impacts of the distribution temperature on the energy and economic performance are investigated in Section 4.3 and Section 4.4, respectively.

4.1. Validation of the system model

Detailed information on the model validation can be found in the paper [46]. This section presents the validation of the bounds of the building model, which described the coupling between the supply and demand sides. Fig. 8 plots the lower bound and the measured supply temperature of the SH system. It shows that the proposed lower bound was consistent with the measurement data. Firstly, the vast majority, about 95%, of the measured supply temperature fell into the area above the lower bound. Secondly, the lower bound presented the same trend as the measured data - the supply temperature decreased with the rising outdoor air temperature. In addition, Fig. 9 presents the measured temperature differences between the supply and return water of the DH system, as well as the regression line obtained using the method provided in Section 2.3. It can be found that the linear regression model could represent the measured data very well, with a coefficient of determination (R^2) of about 0.9.

4.2. Distribution temperature of the four scenarios

This section presents and analyses the simulation results on distribution temperatures. Detailed results on the operating temperatures of the campus DH system, the water flow rate of the campus DH system, and the water temperature developments of the WTTES are presented in Fig B. 1, Fig B. 2, and Fig B. 3 in Appendix B, respectively. The main findings from these results are summarized as follows: 1) for the campus DH system, low supply and low return temperature were preferred and high temperature only existed during the peak periods; 2) for the WTTES during the warm periods, which were from June to October of 2017 and from April to June of 2018, it served to relieve the mismatch, and the charging and discharging processes were controlled based on the states and degree of the mismatch; and 3) for the WTTES during the cold period, which was from October of 2017 to April of 2018, it served to shave the peak load, and the charging process mainly happened at the beginning of the peak periods. The first phenomenon can be explained by that low supply and return temperatures could reduce the distribution heat loss of the campus DH system. The second phenomenon was because the warm period only suffered the mismatch problem and relieving the mismatch could bring heat use saving for the campus DH system. The last phenomenon

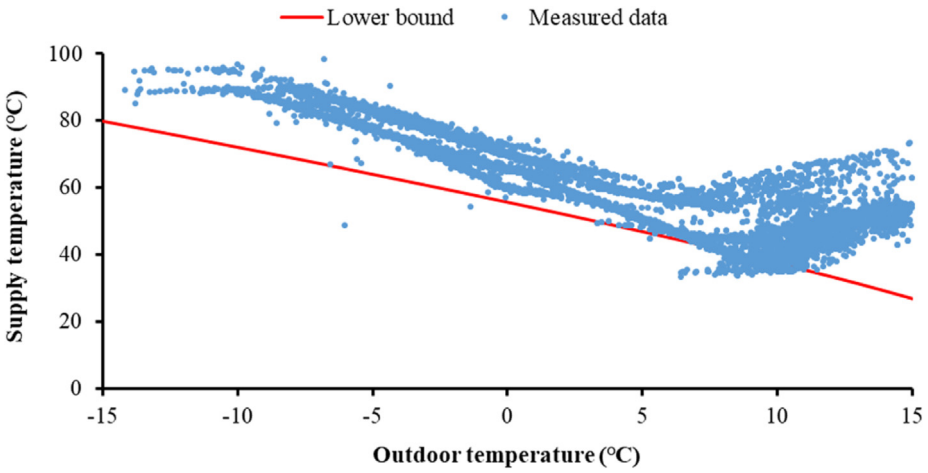

Fig. 8. The lower bound and the measured supply temperature of the SH system.

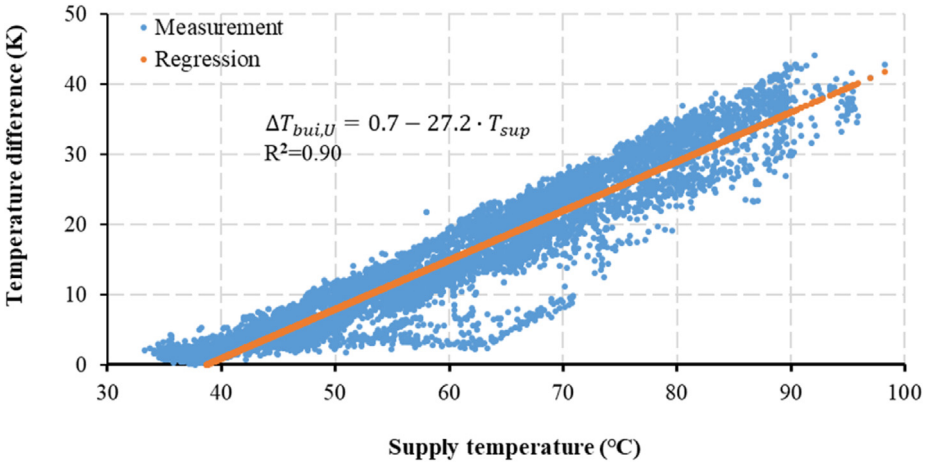

Fig. 9. The measured temperature differences and their regression line.

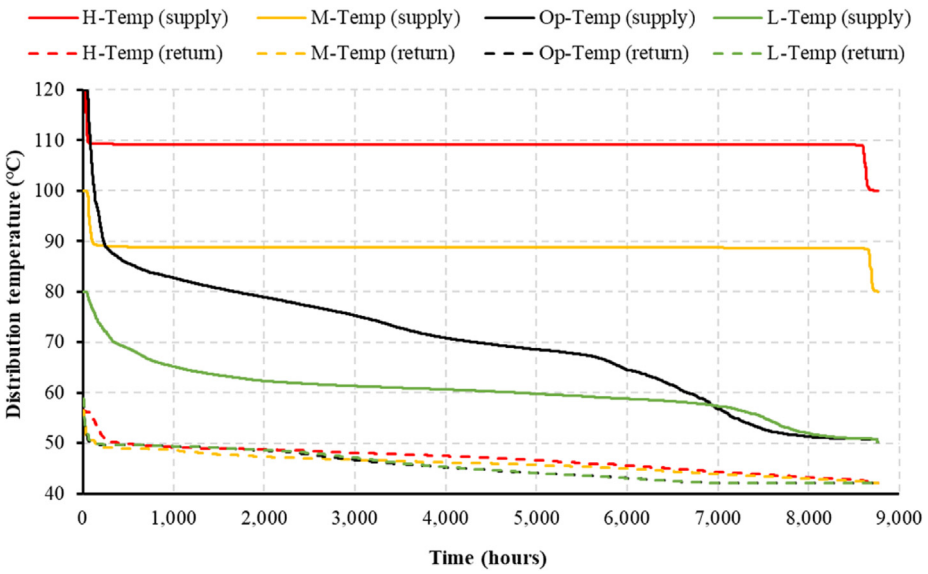

Fig. 10. Distribution temperature duration curves for the four scenarios, the supply temperature is the one with the higher value among the HE1 and HE2's supply temperatures.

appeared due to that charging at the beginning of the peak periods could service for peak load shaving, meanwhile, keeping low storage temperatures during non-peak periods could reduce unnecessary storage heat loss.

The resulting duration curves for the distribution temperatures for the campus DH system are presented in Fig. 10. It can be observed that compared to the benchmark scenarios *H-Temp*, *M-Temp*, and *L-Temp*, the improved scenario *Op-Temp* had the widest distribution range on the supply temperature, ranging from 120 °C to 50 °C and crossing all the benchmark scenarios. This wide distribution can be explained by that the scenario *Op-Temp* took full advantage of its high flexibility on the supply temperature to obtain the optimal economic performance. The return temperature, on the other hand, showed minimal variation among scenarios with the same distribution range of 40 °C–60 °C.

The resulting annual average distribution temperatures of the campus DH system are presented in Fig. 11. It can be found that the annual average supply temperatures varied substantially between scenarios, ranging from 109 °C to 59 °C. However, the return temperature had very close annual average values about 45 °C in all scenarios. Furthermore, the economic optimal distribution temperature achieved by the scenario *Op-Temp* differed considerably from the lowest distribution temperature obtained by the scenario *L-Temp*. The former's supply temperature was 70 °C, 11 °C higher than the latter's 59 °C.

4.3. Impacts of distribution temperature on energy performances

This section analyses the impacts of distribution temperature on energy performances, including peak load and heat use. Analysis in Section 4.2 shows that distribution temperatures can be distinguished by their supply temperatures. Therefore, figures hereinafter sort the scenarios based on the annual average supply temperature, from the highest to the lowest, i.e., with the order *H-Temp*, *M-Temp*, *Op-Temp*, and *L-Temp* from the left side to the right side.

The heat flow rates of the campus DH system are presented in Fig. B.4 in Appendix B, the corresponding heat load duration curves are presented in Fig. 12, and the resulting peak loads are presented in Fig. 13. Results showed that for the benchmark scenarios, the decreasing distribution temperature reduced the peak load shaving effect of WTTES, and thus increased the peak load. As shown by the area highlighted with red colour in Fig. 12 and the columns in Fig. 13, the peak load of the benchmark scenarios presented a rising trend from 10.8 MW to 11.5 MW from the scenarios *H-Temp* and *M-Temp* to the scenario *L-Temp*. However, this reduced peak load shaving effect was effectively avoided by the improved scenario *Op-Temp* by using the optimal distribution temperature. Even with a lower distribution temperature, the peak load of Scenario *Op-Temp* was around 10.5 MW, which was the lowest of all the scenarios.

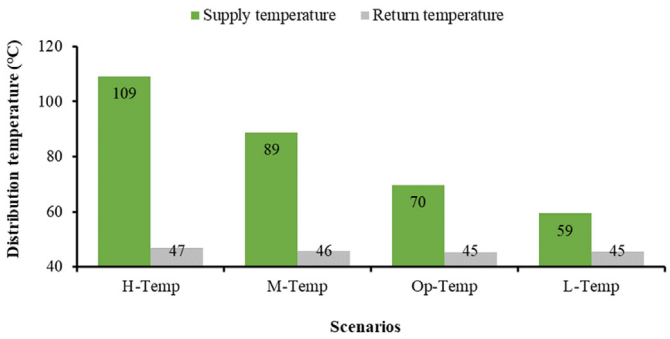

Fig. 11. Annual average distribution temperatures of the four scenarios, scenarios were sorted based on the annual average supply temperature from the highest to the lowest from the left side to the right side.

The heat use of the campus DH system depended on three aspects: heat loss from the WTTES, heat loss from the pipeline, and waste heat utilization of the DC. The conditions of these aspects of the four scenarios are presented in Fig. 14. It was discovered that the distribution temperature had a minor impact on the heat loss of WTTES, with an annual heat loss of 0.2 GWh for all the scenarios. It was because these scenarios kept a similar low storage temperature during most of the year (non-peak periods) as explained in Section 4.2. However, the results suggested that lowering the distribution temperature considerably decreased the pipeline's heat loss. The pipeline's heat loss was reduced from 6.7 GWh to 5.9 GWh from the high-temperature scenario *H-Temp* to the low-temperature scenario *L-Temp*. The significant share of distribution heat loss, which was around 20% of the delivered heat, was responsible for this remarkable decrease. In terms of the DC's waste heat utilization, the distribution temperature played a minimal role. For all four scenarios, the annual utilized waste heat was 8.8 GWh. This less important role was because, as mentioned in Section 4.2, the four scenarios exhibited slight differences in return temperature, which impacted the DC's waste heat recovery. In addition, the R2R connection may limit the amount of waste heat utilization, and different results may be obtained for other types of connection [40].

The resulting annual heat use for the four scenarios is shown in Fig. 15. It can be found that the total annual heat use decreased from 31.1 GWh to 30.4 GWh with the decreasing distribution temperature. Moreover, the scenario with the economic optimal distribution temperature, *Op-Temp*, had the least heat use, which was the same as the scenario with the lowest distribution temperature *L-Temp*.

4.4. Impacts of distribution temperature on economic performances

This section analyses the impacts of distribution temperature on economic performances in terms of the heating cost. The currency in this section was in NOK.[1] As introduced in Section 2.2, heating cost included two parts: the LDC heating cost, which was determined by the peak load; and the EDC heating cost, which depended on the heat use. The annual heating costs for the four scenarios are presented in Fig. 16.

Results showed that the decreasing distribution temperature increased the annual LDC heating cost for the benchmark scenarios. The annual LDC heating cost of the benchmark scenarios presented a rising trend from 4.6 million NOK to 4.9 million NOK from the high-temperature scenario *H-Temp* to the low-temperature scenario *L-Temp*. However, this rising trend was effectively avoided by the improved scenario *Op-Temp* by using the optimal distribution temperature. Even with a lower distribution temperature, the annual LDC heating cost for the scenario *Op-Temp* was 4.5 million NOK, which was the lowest of all the scenarios. The obtained results on the annual LDC heating cost can be explained by the conditions of the peak load observed in Section 4.3 because they were positively correlated. In addition, the annual EDC heating cost decreased from 18.2 million NOK to 17.7 million NOK with the decreasing distribution temperature. Meanwhile, the scenario with the economic optimal distribution temperature, *Op-Temp*, had the lowest annual EDC heating cost, which was the same as the scenario with the lowest distribution temperature *L-Temp*. Similarly, the obtained results on the annual EDC heating cost can be explained by the conditions of annual heat use observed in Section 4.3 because of the positive correlation between them.

[1] The currency rate between NOK and EUR can be found from https://www.xe.com/, in this study 1 EUR = 10 NOK.

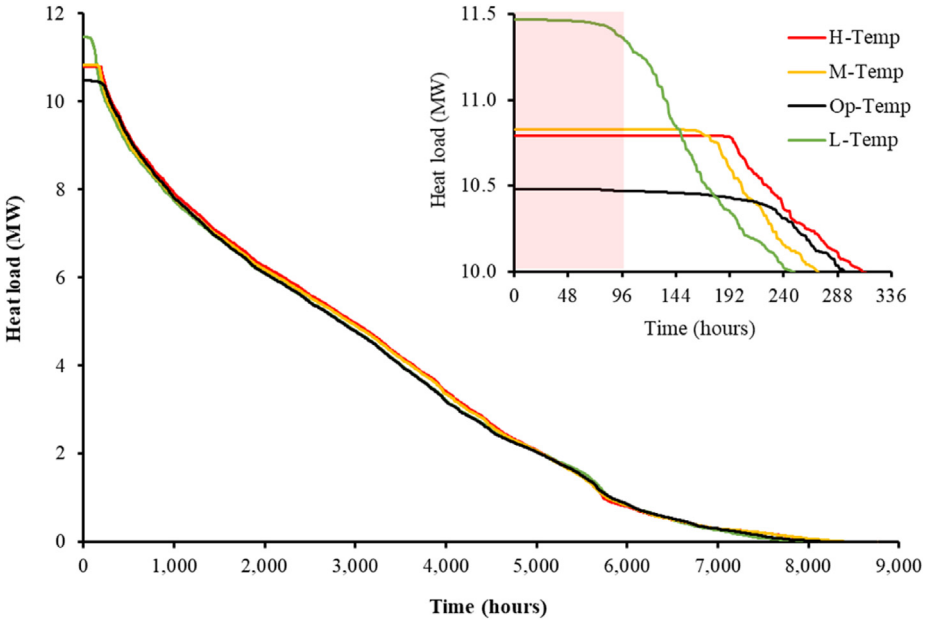

Fig. 12. Heat load duration diagram for the four scenarios.

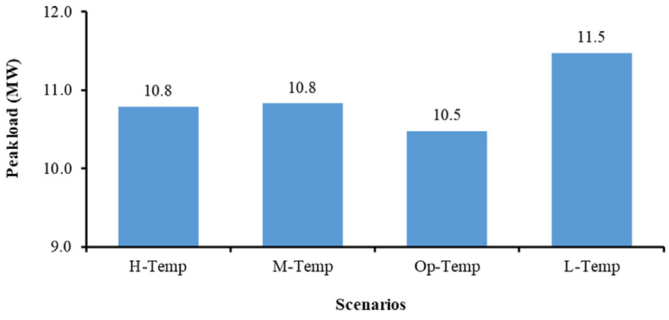

Fig. 13. Peak load for the four scenarios.

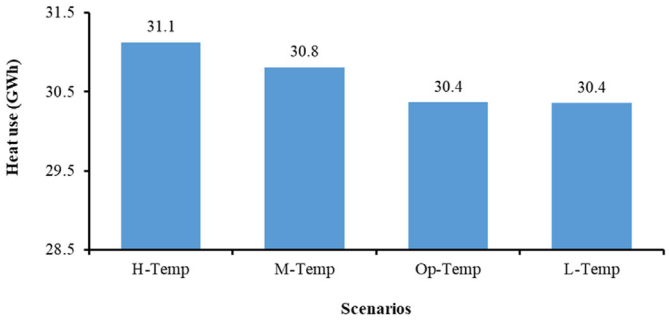

Fig. 15. Annual heat use for the four scenarios.

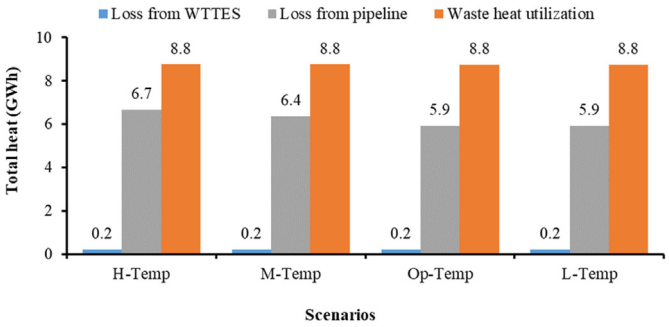

Fig. 14. Annual heat loss and waste heat utilization of the four scenarios.

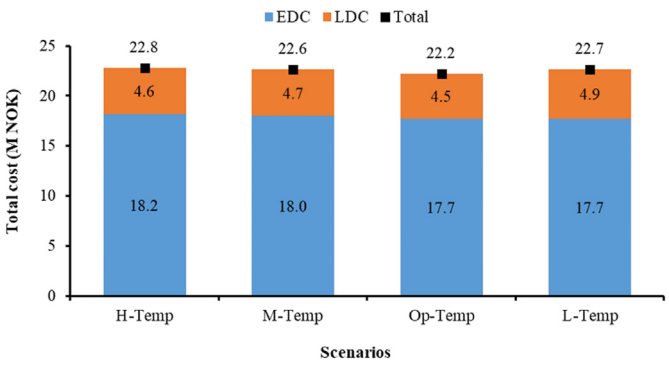

Fig. 16. Annual total heating cost for the four scenarios.

The resulting annual total heating cost of the four scenarios is also presented in Fig. 16. As shown in Fig. 16, the scenario with the economic optimal distribution temperature, *Op-Temp*, achieved the best performance with the lowest annual total heating cost of 22.2 million NOK. The scenario with the medium distribution temperature, *M-Temp*, followed this performance with a higher annual total heating cost of 22.6 million NOK. In contrast, the high-temperature scenario *H-Temp* and the low-temperature scenario *L-Temp* had the highest annual total heating costs of 22.8 and 22.7 million NOK, which were 0.6 and 0.4 million NOK higher than the scenario *Op-Temp*, accounting for an increase of 2% and 3%, respectively.

5. Discussion

The impacts of TES's storage capacity and DHS's renewable fraction (RF) are discussed first in this section to reach more broad

study findings on economic optimal distribution temperature, followed by the effects of heating price models and heat density. Finally, the limitations of the work are acknowledged, along with suggestions for further research.

5.1. Impacts of TES's storage capacity and DHS's RF

This section discusses the impacts of two crucial factors: the storage capacity of TES and the RF of DHS. The first one is a key factor determined in the system design process, while the second one reflects the availability of renewable energies. As described in Table A. 1, the storage capacity of WTTES in Section 4 was 12 h, i.e., being capable to supply heat continually for 12 h under a discharging heat flow rate that was equal to the annual average heat demand. This storage capacity made a trade-off between the investment of WTTES and the reduction of operating costs [46]. However, owing to shifting circumstances, such as changes in available investment and variations in expected operating costs, heat prosumers may choose different storage capacities. In addition, heat prosumers may have different RFs, an indicator showing the percentage of heat demand covered by renewable energies. For solar DH systems, for example, RFs of 10–50% are technologically and economically viable, and a theoretical RF of 100% is even possible [56].

To investigate the impacts of the above factors on heat prosumers' economic optimal distribution temperature, further scenarios were introduced as presented in Table 2. The benchmark scenario was identical to the improved scenario *Op-Temp* in Section 4, with a storage capacity of 12 h, a DC capacity (maximum waste heat recovery flow rate) of 1.0 MW, and an RF of 27%. In comparison to the benchmark scenario, the TES scenarios altered the storage capacity ranging from 6 to 120 h (a quarter to five days), whereas the DHS scenarios modified the RF ranging from 13% to 100%. The TES and DHS scenarios were created by changing the volume of WTTES and adjusting the capacity of DC, respectively.

The annual average distribution temperatures of the TES and DHS scenarios are presented in Fig. 17 and Fig. 18, respectively. Fig. 17 shows that scenarios with larger WTTES tend to have higher economic optimal supply temperatures. It can be explained by Fig. C. 1 in Appendix C that it was caused by the higher charging temperatures during the peak load periods. Furthermore, as shown in Fig. C. 2 in Appendix C, scenarios with larger WTTES took advantage of the higher charging temperatures to achieve greater peak load shaving effects from their WTTESs.

Fig. 18 shows that scenarios with lower RF tend to have slightly higher economic optimal supply temperatures and lower return temperatures. It can be explained by Fig. C. 3 in Appendix C that the higher supply temperatures were caused by the higher charging

Table 2
Information for the scenarios.

Abbreviation	TES (WTTES)			DHS (DC)		
	Scale	Capacity	Volume	Scale	RF	Capacity
	(1)	(hour)	(m^3)	(1)	(%)	(MW)
Benchmark scenario						
Ref	1	12	900	1	27	1.0
TES scenarios						
TES 1/2	1/2	6	400	1	27	1.0
TES 2	2	24	1700	1	27	1.0
TES 6	6	72	5200	1	27	1.0
TES 10	10	120	8600	1	27	1.0
DHS scenarios						
DHS 1/2	1	12	900	1/2	13	0.5
DHS 2	1	12	900	2	53	2.0
DHS 3	1	12	900	3	80	3.0
DHS 4	1	12	900	4	100	4.0

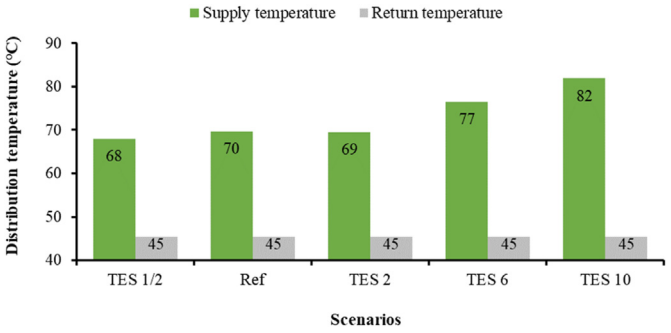

Fig. 17. Annual average distribution temperatures of the benchmark and TES scenarios.

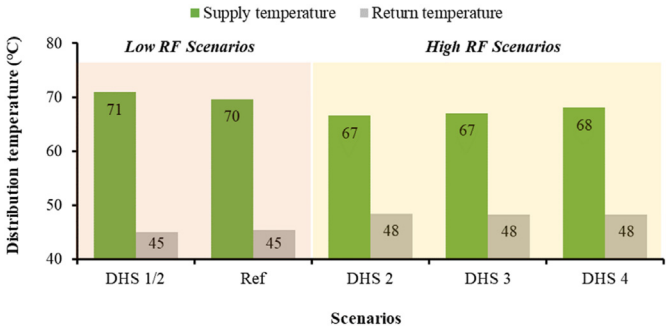

Fig. 18. Annual average distribution temperatures of the benchmark and DHS scenarios.

and boosting temperatures during the mismatch problem periods. Meanwhile, the lower return temperatures were the result of the higher supply temperatures, i.e., as shown in Fig. 9, a higher supply temperature would make it possible for greater temperature difference and lower return temperature. Furthermore, as shown in Fig. C. 4 in Appendix C, scenarios with lower RF used those higher supply temperatures to obtain more heat supply from the MS, compensating for the less renewable heat available from the DHS.

5.2. Impacts of heating price model and heat density

This section discusses the impacts of two other crucial factors: the share of LDC heating cost and the linear heat density of a DH system. The first one is an economic factor that reflects the impact of peak load on total heating costs, while the second one is a technical factor that influences the distribution heat loss of DH systems. As introduced in Section 2, the share of LDC heating cost ranges from 0% to 50% depending on heating price models. This study presented a medium level of 20–22%, which was close to the average level of 28% observed from the survey on heating pricing models in Sweden [34]. Raising the share of the LDC heating cost motivates heat users to shave their peak load, and thus increases the economic optimal distribution temperature because TESs need higher charging temperatures to achieve larger peak load shaving capacities.

Moreover, as identified by Ref. [29], the distribution heat loss of a DH system depends on four factors: distribution temperature, pipe diameter, the heat transmission coefficient of insulation, and linear heat density. The most important factor is the linear heat density due to its great variation among DH systems [29]. This study had a linear heat density of 2 MWh/(m·a), which was within the average range from 2 MWh/(m·a) to 4 MWh/(m·a) for DH systems in Sweden. Decreases in linear heat density would be

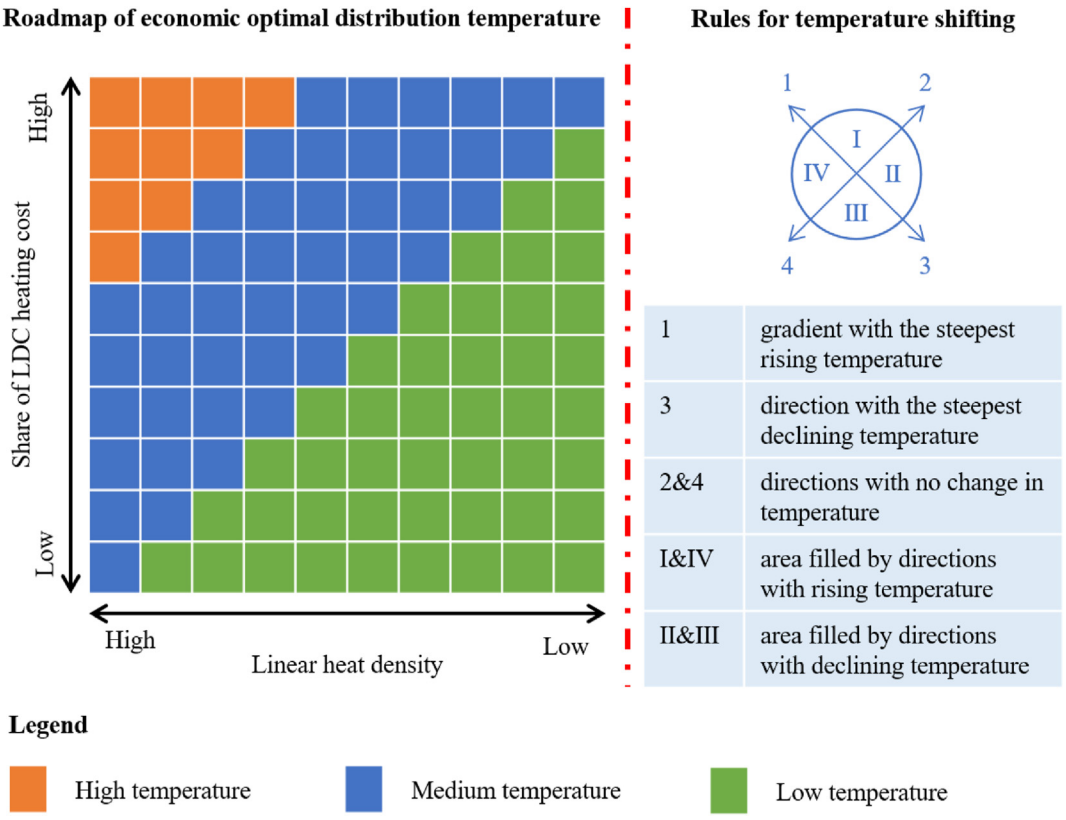

Fig. 19. Roadmap for the economic optimal distribution temperature.

detrimental to heat distribution and result in higher distribution heat loss, consequently, the economic optimal distribution temperature should be reduced to maintain the same level of the heating cost.

Based on the above analysis, the left side of Fig. 19 is made to map the correlations between the economic optimal distribution temperature and the mentioned economic and technical factors. The orange rectangles in the upper left corner and the green rectangles in the bottom right corner locate the situations with high and low economic optimal distribution temperatures, respectively. As introduced in Section 1, the current DH systems mainly use hot water as the medium, therefore the high and low distribution temperatures in Fig. 19 may belong to the 2nd and 4th generation DH system, respectively. The blue rectangles represent the situations with medium economic optimal distribution temperatures, which may belong to the 3rd generation DH system. It is difficult to point out the exact economic optimal distribution temperature for a DH system under a certain condition without detailed research, however, some general rules can be deduced regarding the trend for the temperature shifting as illustrated on the right side of Fig. 19. The mentioned two factors drive the shifting of the economic optimal distribution temperature, and the overall driven force determines the final shifting effect. Any condition changes towards the upper left directions would raise the economic optimal distribution temperature, while changes in the opposite directions would decrease it.

5.3. Limitation and future work

Firstly, the optimization problem in Section 2.2 only applies to the heat pricing models that calculate the LDC heating cost using the measured peak load. However, DH companies may use another variable, i.e. flow capacity, to calculate the LDC heating cost instead of peak load [29,57]. The flow capacity is obtained by dividing the heat use over a certain period by a predefined category number [57]. However, due to the installation of smart meters and the trend of digitalization, an increasing number of DH companies are starting to utilize real-time measurement for charging heat bills. Therefore, the developed method in this research adopted the heat pricing models using the measured peak load to calculate heat users' LDC heating cost.

Secondly, thermal couplings between the supply and demand sides should be handled more meticulously by the optimization problem. To represent these thermal couplings, the optimization problem in Section 2.3 used a simplified technique, i.e., utilizing bounds to constrain the supply side's supply water temperature and temperature difference. To some extent, using bounds to constrain these temperatures, however, is insufficient to describe the thermal couplings. These couplings are the results of a complicated heat transfer process that is influenced by operating variables on both sides. Nonlinear equations may be required to describe this process, such as using the Number of Thermal Units Method. These nonlinear equations, on the other hand, may reduce computationally efficiency and cause numerical instabilities for the optimization problem. Moreover, obtaining the variables on the demand side used by these nonlinear equations, which must consider weather conditions as well as thermal dynamics of buildings and heating systems, may further increase the complexity of the optimization problem. In the future, a more precise and effective method of describing these thermal couplings will be developed.

6. Conclusions

This study aimed to economically optimize the distribution temperature of heat-prosumer-based DH systems with short-term

TESs. Moreover, it made a pioneering effort to distinguish the economic optimal distribution temperature from the lowest distribution temperature for DH systems. Four scenarios with different distribution temperature levels were designed, including three benchmark scenarios *H-Temp*, *M-Temp*, and *L-Temp* representing the 2nd, 3rd, and 4th generation DH systems, respectively, and an improved scenario *Op-Temp* with high flexibility in distribution temperature. The following conclusions were obtained.

Firstly, the economic optimal distribution temperature achieved by Scenario *Op-Temp* differed considerably from the lowest distribution temperature obtained by Scenario *L-Temp*. The former one had an annual average supply temperature of 70 °C, which was higher than the latter one of 59 °C.

Secondly, for the benchmark scenarios, the peak-load-related heating cost, LDC, presented a rising trend with the decreasing distribution temperature, which was increased from 4.6 million NOK to 4.9 million NOK from the high-temperature scenarios, *H-Temp*, to the low-temperature scenario, *L-Temp*. However, the heat-use-related heating cost, EDC, showed an opposite trend, i.e., it decreased from 18.2 million NOK to 17.7 million NOK with the decreasing distribution temperature.

Thirdly, the improved scenario, *Op-Temp*, achieved the economic optimal distribution temperature, with the lowest annual heating costs on LDC, EDC, and the total. It saved 0.4–0.6 million NOK total heating costs per year, accounting for a cost saving of 2–3% compared to the benchmark scenarios.

Finally, studies on the impacts of crucial factors revealed that the economic optimal supply temperature would be lowered when increasing the renewable share, while the economic optimal supply temperature would be raised when increasing the TES's storage capacity, the linear heat density, and the proportion of the LDC heating cost.

This study improved the understanding of the temperature development of DH systems and supported the transition towards the future completely renewable-based DH systems, especially for heat-prosumer-based DH systems with TESs.

Credit author statement

Haoran Li: Conceptualization, Methodology, Software, Validation, Writing – original draft. **Juan Hou:** Conceptualization, Methodology, Writing – original draft. **Tianzhen Hong:** Writing – review & editing. **Natasa Nord:** Writing – review & editing, Supervision.

Declaration of competing interest

The authors declare that they have no known competing financial interests or personal relationships that could have appeared to influence the work reported in this paper.

Acknowledgement

The authors gratefully acknowledge the support from the Research Council of Norway through the research project Understanding behaviour of district heating systems integrating distributed sources under the FRIPRO/FRINATEK program (project number 262707) and the innovation project Low-temperature thermal grids with surplus heat utilization under the EnergiX program (project number 280994).

Appendix A. Simulation settings

Table A. 1
Key parameter setting for the simulation.

Category	Parameter	Value
WTTES	*Storage capacity*	12 h
	Tank volume	900 m^3
	Tank diameter	8.7 m
	Tank height	15 m
Pipeline	*Route length*	15,000 m
	Pipe diameter	0.273 m
	Ground heat conductivity	1.5 W/(m·K)
	Insulation heat conductivity	0.03 W/(m·K)
Heating price	*EP(t)*	see Fig A. 1
	LP	33 NOK/kW/month

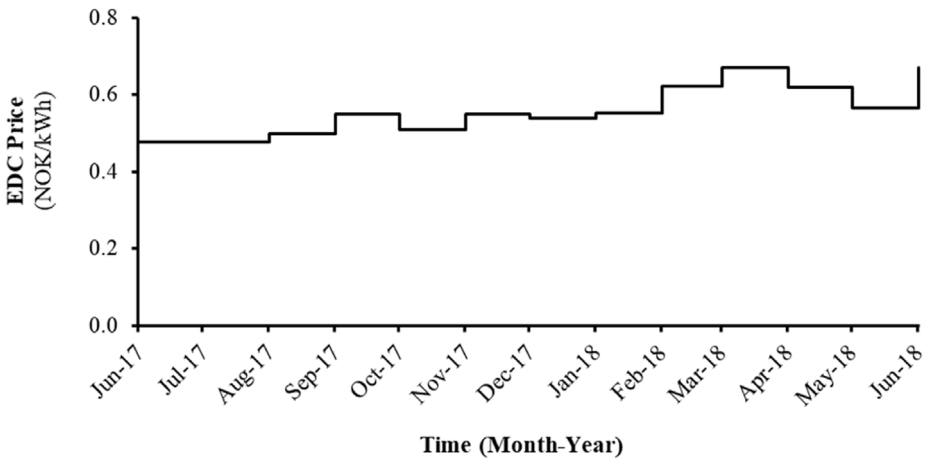

Fig. A. 1. The EDC heating price [58].

Appendix B. Simulation results

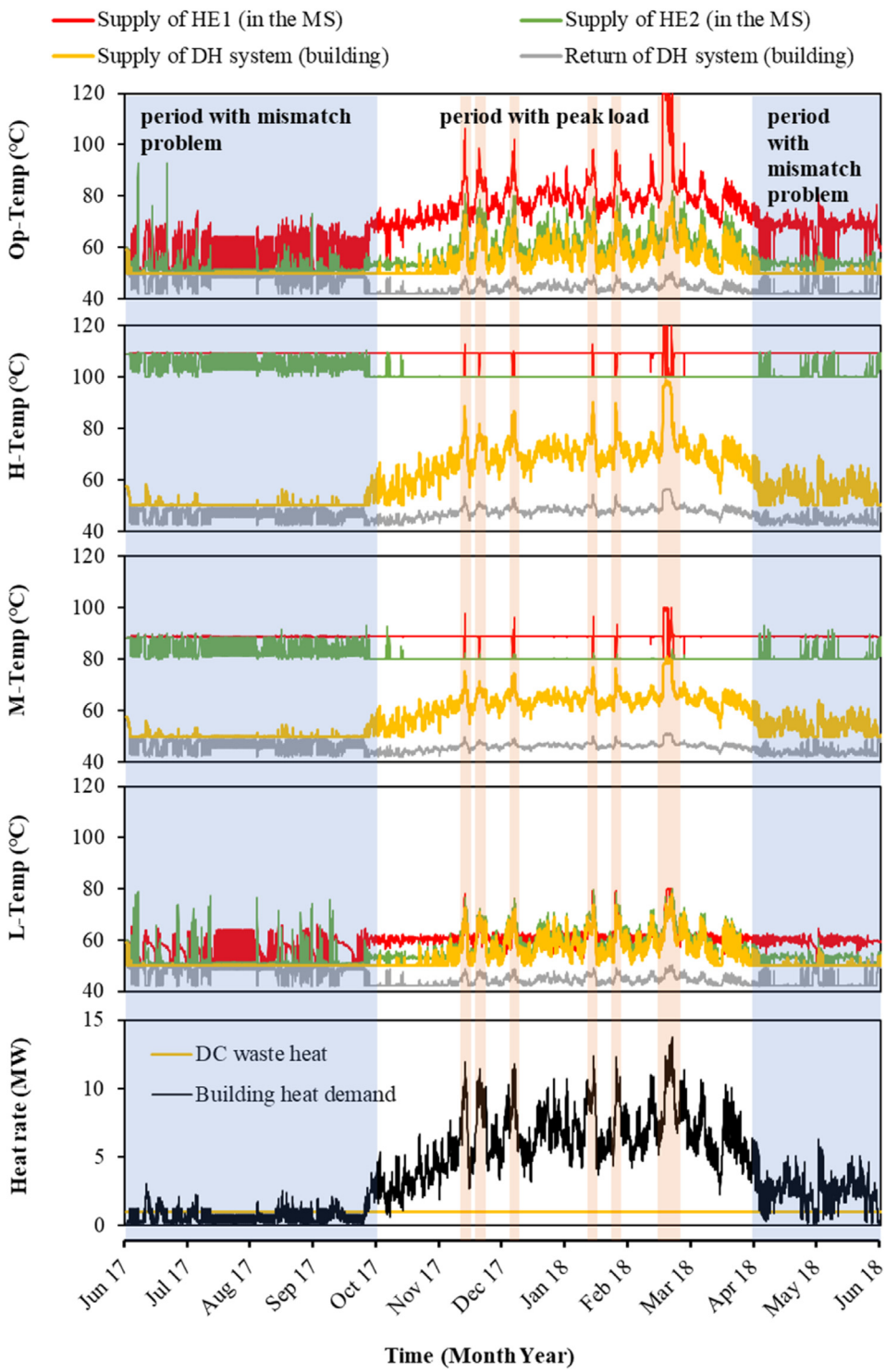

Fig. B. 1. Operating temperatures of the campus DH system.

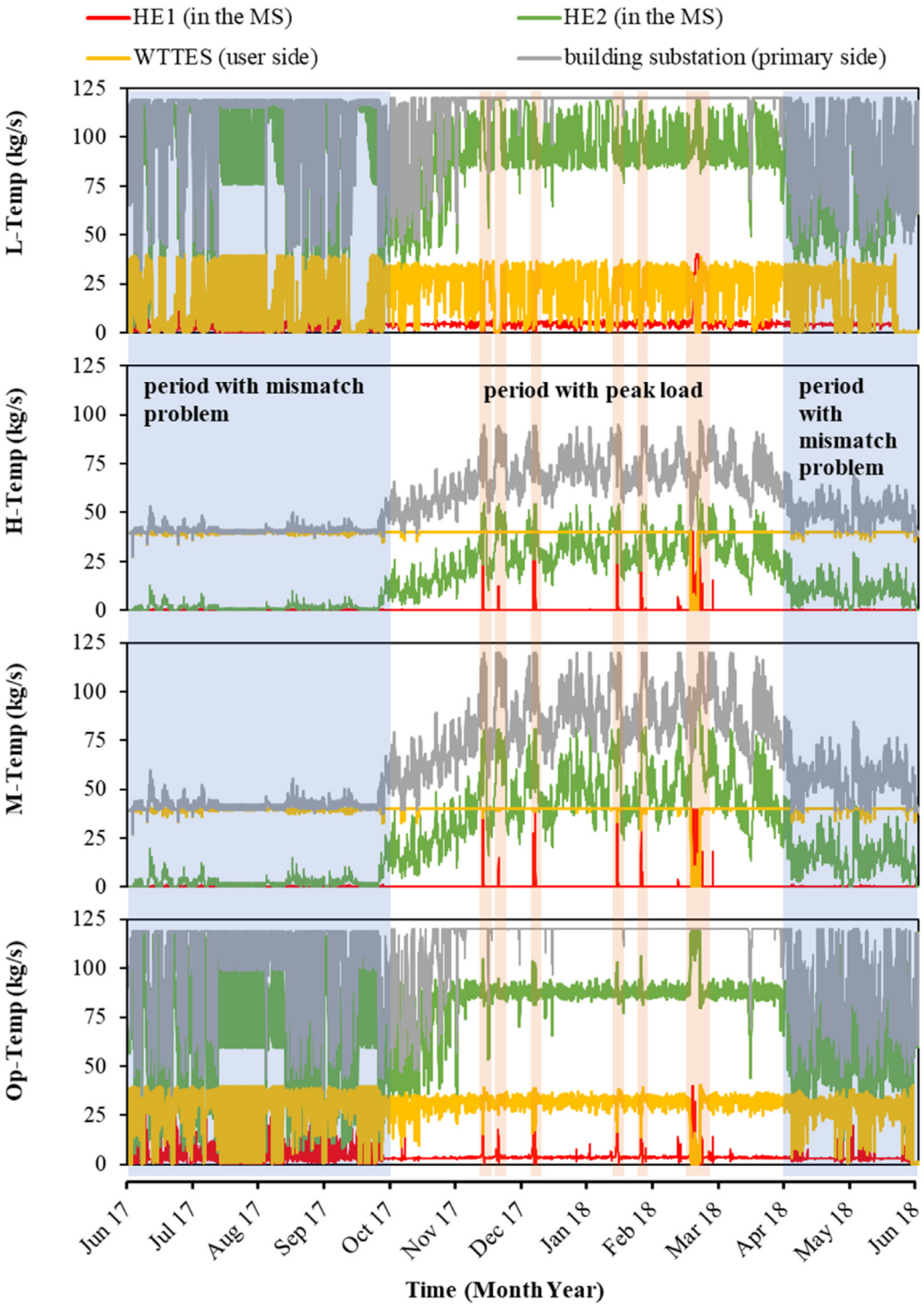

Fig. B. 2. Water flow rate of the campus DH system.

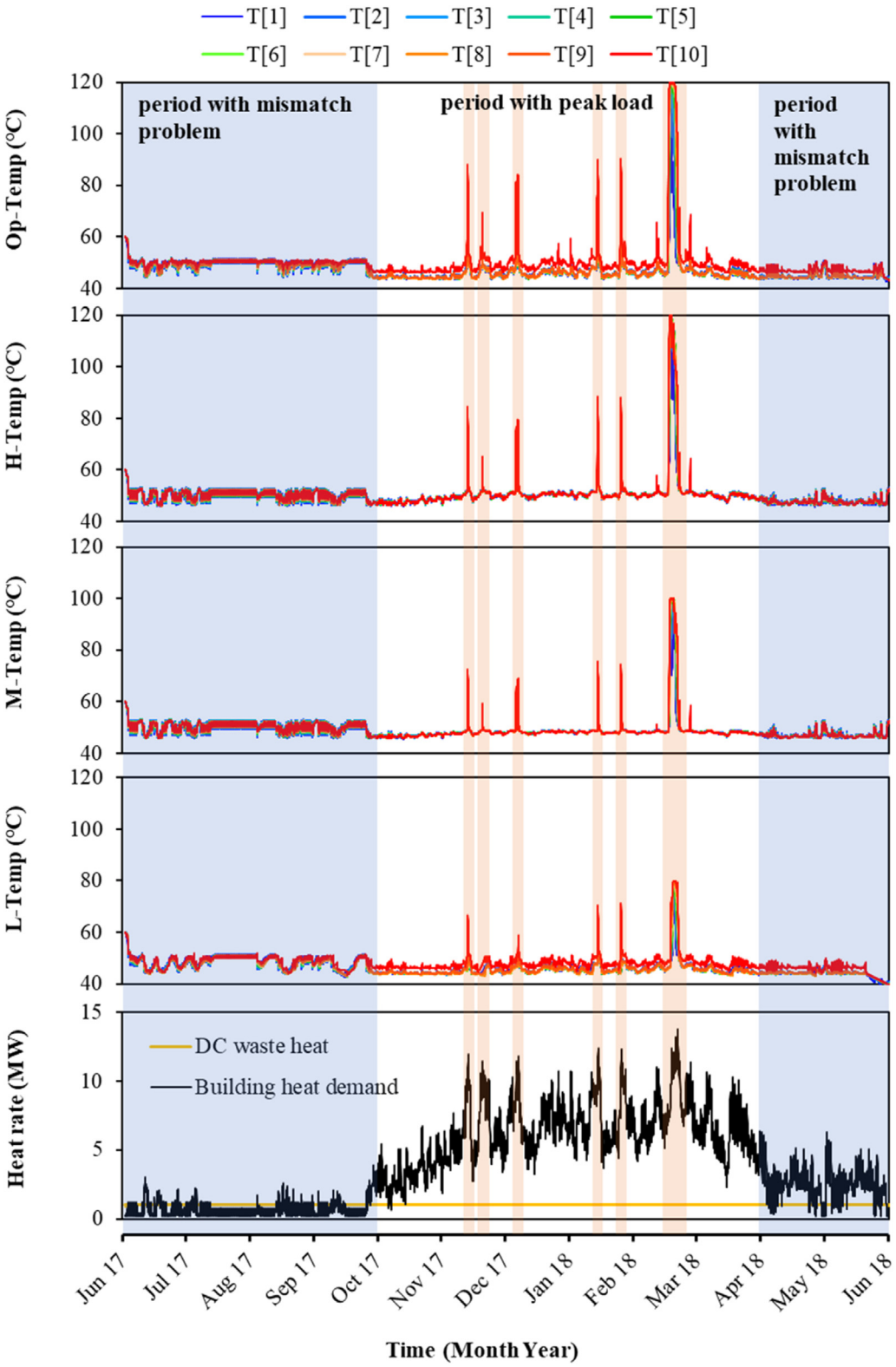

Fig. B. 3. Water temperature developments of the WTTES layers.

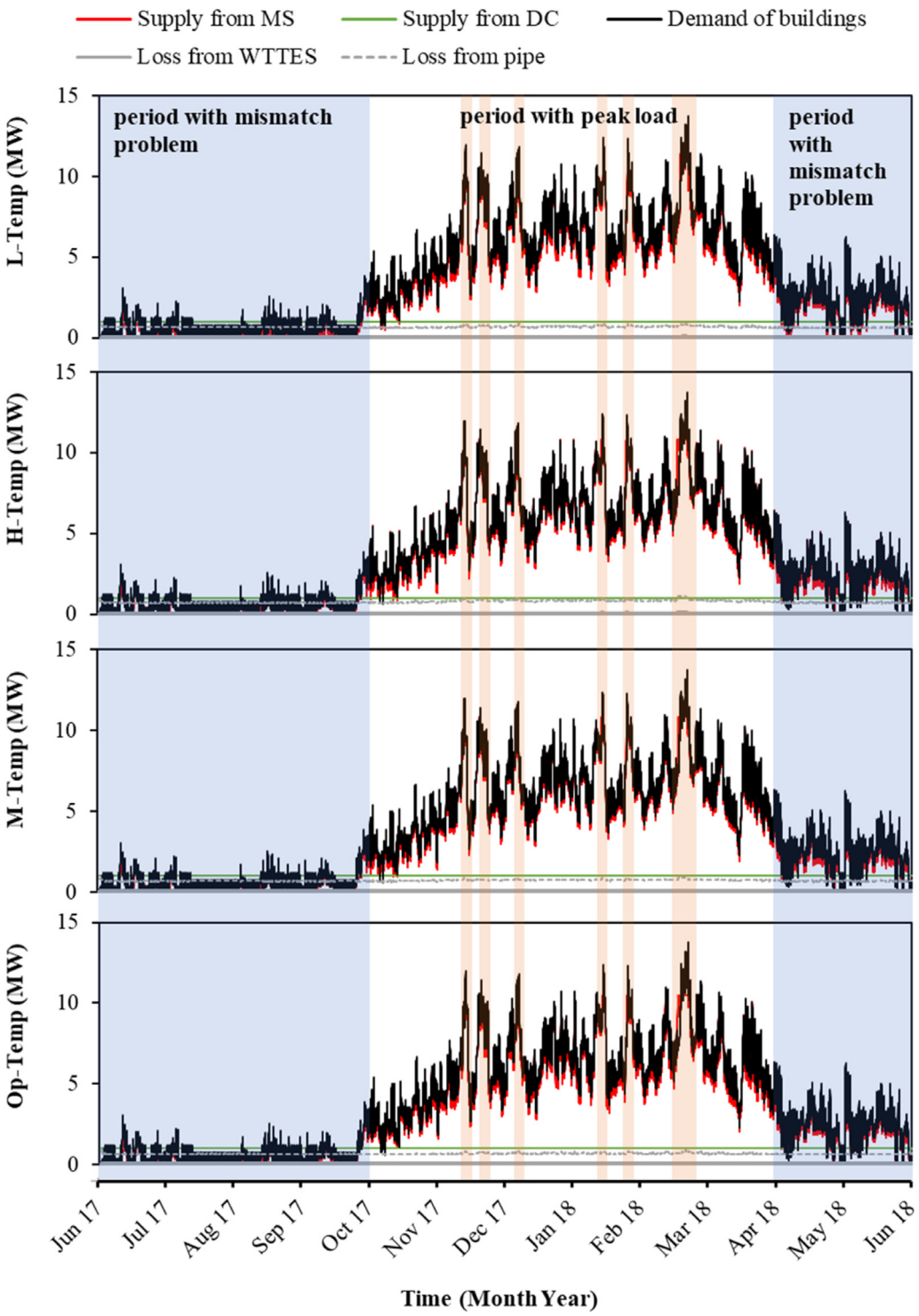

Fig. B. 4. Heat flow rate of the campus DH system.

Appendix C. Simulation results for the discussion

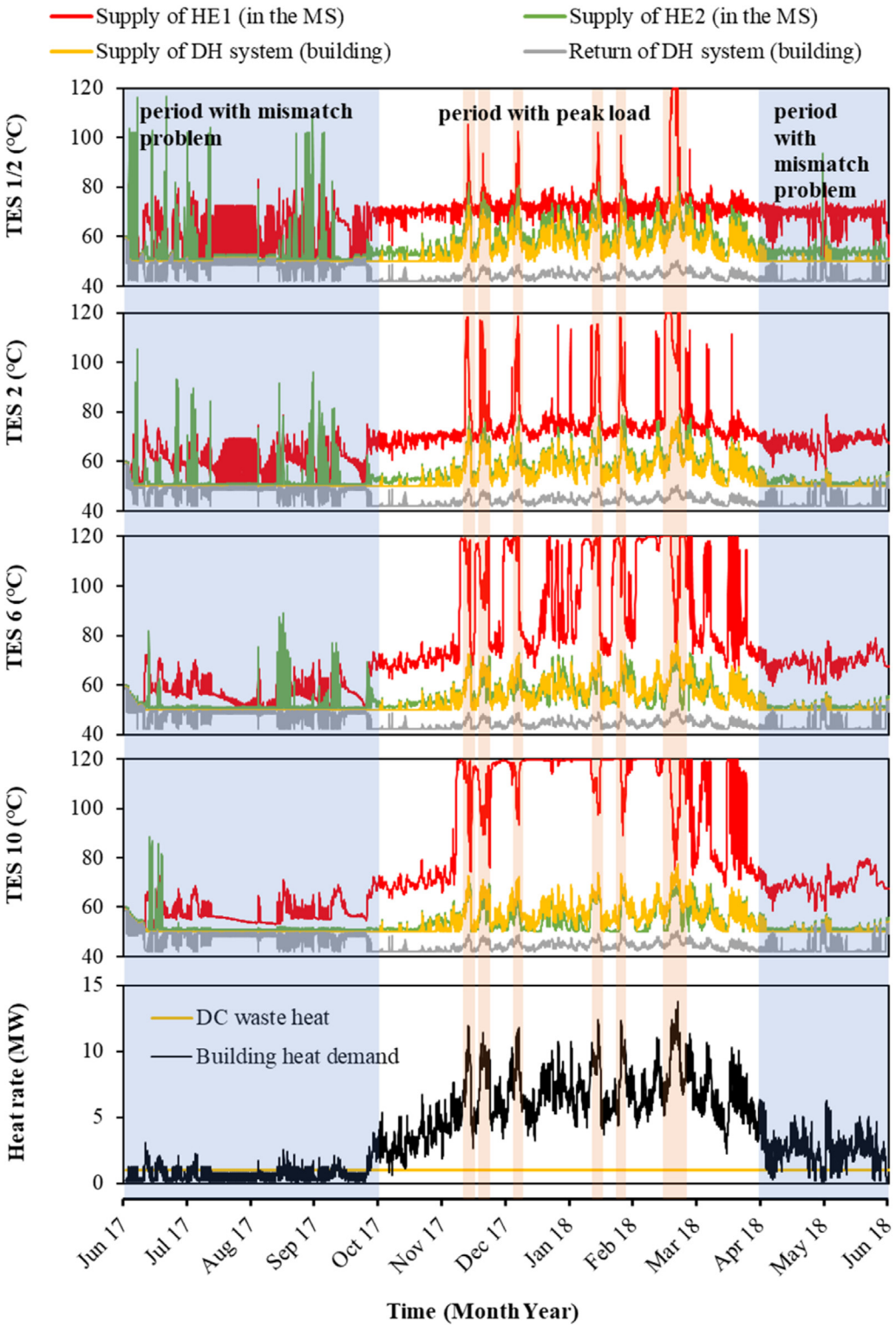

Fig. C. 1. Operating temperatures of the campus DH system for the TES scenarios.

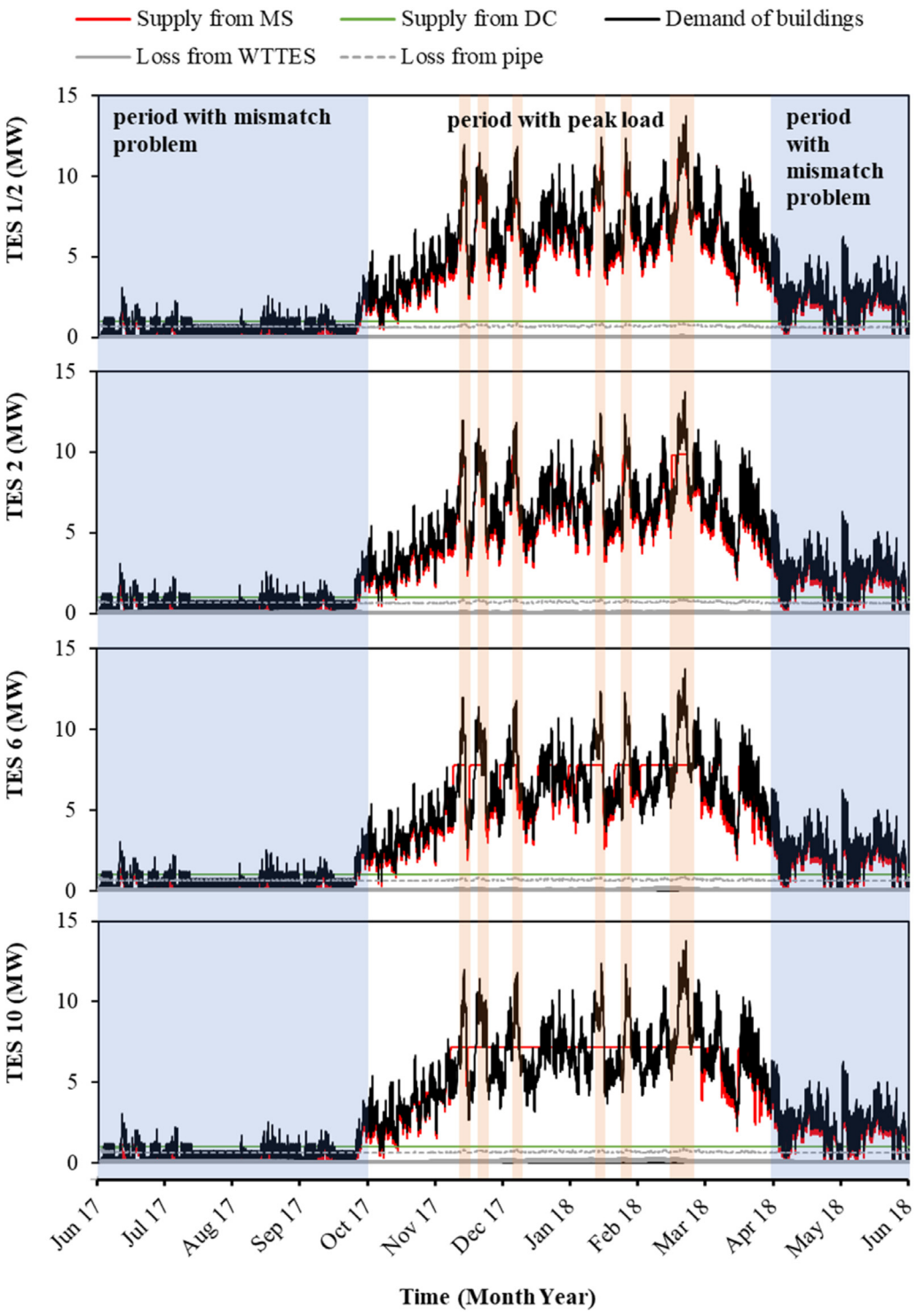

Fig. C. 2. Heat flow rate of the campus DH system for the TES scenarios.

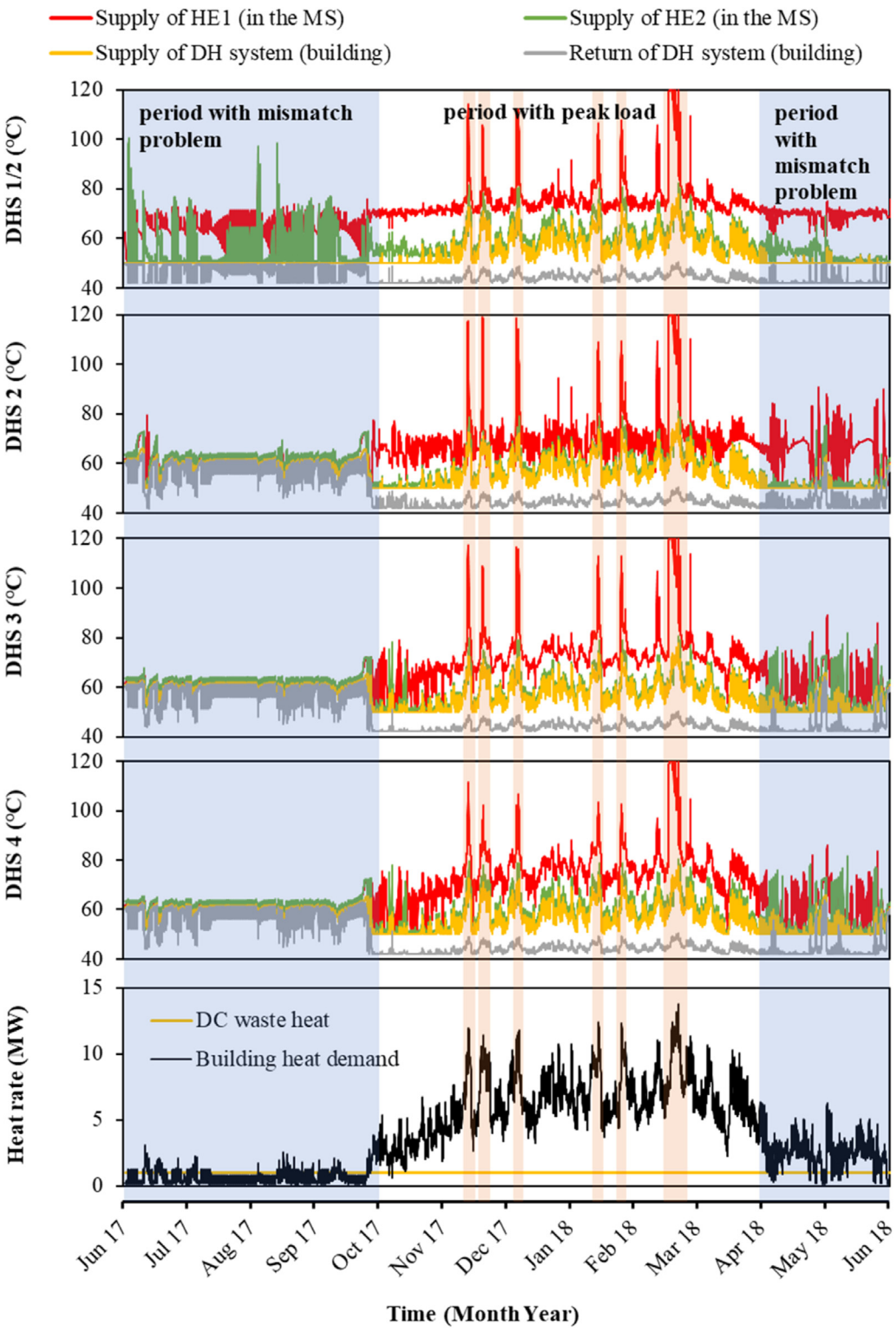

Fig. C. 3. Operating temperatures of the campus DH system for the DHS scenarios.

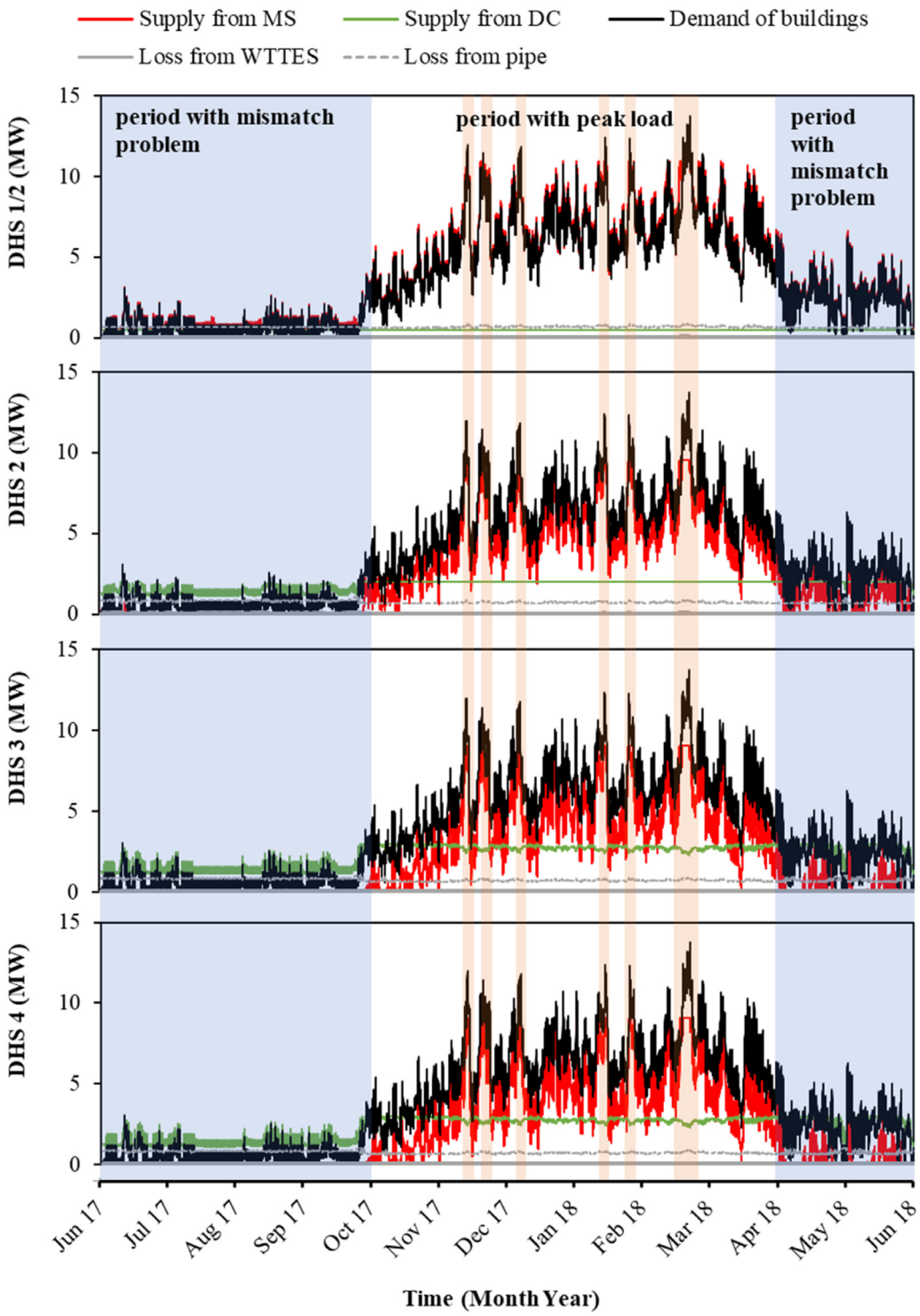

Fig. C. 4. Heat flow rate of the campus DH system for the DHS scenarios.

References

[1] In focus: Energy efficiency in buildings. https://ec.europa.eu/info/news/focus-energy-efficiency-buildings-2020-feb-17_en#:∼:text=Collectively%2C%20buildings%20in%20the%20EU,%2C%20usage%2C%20renovation%20and%20demolition. [Accessed September 2020].

[2] Heating and cooling. https://ec.europa.eu/energy/topics/energy-efficiency/heating-and-cooling_en?redir=1. [Accessed September 2020].

[3] Mapping and analyses of the current and future. heating/cooling fuel deployment (fossil/renewables). 2020-2030. https://ec.europa.eu/energy/studies/mapping-and-analyses-current-and-future-2020-2030-heatingcooling-fuel-deployment_en. [Accessed September 2020].

[4] Li H, Nord N. Transition to the 4th generation district heating- possibilities, bottlenecks, and challenges. Energy Proc 2018;149:483–98.

[5] Werner S. International review of district heating and cooling. Energy 2017;137:617–31.

[6] Åberg M, Fälting L, Lingfors D, Nilsson AM, Forssell A. Do ground source heat pumps challenge the dominant position of district heating in the Swedish heating market? J Clean Prod 2020;254:120070.

[7] Connolly D, Lund H, Mathiesen BV, Werner S, Möller B, Persson U, et al. Heat Roadmap Europe: combining district heating with heat savings to decarbonise

the EU energy system. Energy Pol 2014;65:475–89.
[8] Christian Holmstedt Hansen OG, Hanne Kortegaard Støchkel, Detlefsen Nina. The competitiveness of district heating compared to individual heating. 2018.
[9] Dalla Rosa A, Li H, Svendsen S, Werner S, Persson U, Ruehling K, et al. IEA DHC Annex X report: toward 4th generation district heating. In: Experience and potential of low-temperature district heating; 2014.
[10] Persson U, Werner S. Heat distribution and the future competitiveness of district heating. Appl Energy 2011;88(3):568–76.
[11] Lund H, Werner S, Wiltshire R, Svendsen S, Thorsen JE, Hvelplund F, et al. 4th Generation District Heating (4GDH): integrating smart thermal grids into future sustainable energy systems. Energy 2014;68:1–11.
[12] Østergaard DS, Svendsen S. Costs and benefits of preparing existing Danish buildings for low-temperature district heating. Energy 2019;176:718–27.
[13] Averfalk H, Werner S. Economic benefits of fourth generation district heating. Energy 2020;193:116727.
[14] Hou J, Li H, Nord N. Optimal control of secondary side supply water temperature for substation in district heating systems. 2019.
[15] Li H, Nord N. Operation strategies to achieve low supply and return temperature in district heating system. E3S Web Conf 2019;111:05022.
[16] Hou J, Li H, Nord N, Huang G. Model predictive control under weather forecast uncertainty for HVAC systems in university buildings. Energy Build 2022;257:111793.
[17] Brand M, Svendsen S. Renewable-based low-temperature district heating for existing buildings in various stages of refurbishment. Energy 2013;62:311–9.
[18] Nord N, Ingebretsen M, Tryggestad IS. Possibilities for transition of existing residential buildings to low temperature district heating system in Norway. CLIMA 2016; 2016.
[19] Østergaard DS, Svendsen S. Replacing critical radiators to increase the potential to use low-temperature district heating–A case study of 4 Danish single-family houses from the 1930s. Energy 2016;110:75–84.
[20] Østergaard DS, Svendsen S. Are typical radiators over-dimensioned? An analysis of radiator dimensions in 1645 Danish houses. Energy Build 2018;178:206–15.
[21] Jangsten M, Kensby J, Dalenbäck J-O, Trüschel A. Survey of radiator temperatures in buildings supplied by district heating. Energy 2017;137:292–301.
[22] Østergaard DS, Svendsen S. Experience from a practical test of low-temperature district heating for space heating in five Danish single-family houses from the 1930s. Energy 2018;159:569–78.
[23] Yang X, Li H, Svendsen S. Evaluations of different domestic hot water preparing methods with ultra-low-temperature district heating. Energy 2016;109:248–59.
[24] Baldvinsson I, Nakata T. A feasibility and performance assessment of a low temperature district heating system – a North Japanese case study. Energy 2016;95:155–74.
[25] Volkova A, Krupenski I, Pieper H, Ledvanov A, Latõšov E, Siirde A. Small low-temperature district heating network development prospects. Energy 2019;178:714–22.
[26] Nord N, Løve Nielsen EK, Kauko H, Tereshchenko T. Challenges and potentials for low-temperature district heating implementation in Norway. Energy 2018;151:889–902.
[27] Kauko H, Kvalsvik KH, Rohde D, Hafner A, Nord N. Dynamic modelling of local low-temperature heating grids: a case study for Norway. Energy 2017;139:289–97.
[28] Li H, Svendsen S. Energy and exergy analysis of low temperature district heating network. Energy 2012;45(1):237–46.
[29] Frederiksen S, Werner S. District heating and cooling. Studentlitteratur Lund; 2013.
[30] Lickleder T, Hamacher T, Kramer M, Perić VS. Thermohydraulic model of Smart Thermal Grids with bidirectional power flow between prosumers. Energy 2021;230:120825.
[31] Gross M, Karbasi B, Reiners T, Altieri L, Wagner H-J, Bertsch V. Implementing prosumers into heating networks. Energy 2021;230:120844.
[32] Li H, Hou J, Hong T, Ding Y, Nord N. Energy, economic, and environmental analysis of integration of thermal energy storage into district heating systems using waste heat from data centres. Energy 2021;219:119582.
[33] Huang P, Copertaro B, Zhang X, Shen J, Löfgren I, Rönnelid M, et al. A review of data centers as prosumers in district energy systems: renewable energy integration and waste heat reuse for district heating. Appl Energy 2020;258:114109.
[34] Song J, Wallin F, Li H. District heating cost fluctuation caused by price model shift. Appl Energy 2017;194:715–24.
[35] Verda V, Colella F. Primary energy savings through thermal storage in district heating networks. Energy 2011;36(7):4278–86.
[36] Harris M. Thermal energy storage in Sweden and Denmark: potentials for technology transfer. Master thesis; 2011.
[37] Verrilli F, Srinivasan S, Gambino G, Canelli M, Himanka M, Del Vecchio C, et al. Model predictive control-based optimal operations of district heating system with thermal energy storage and flexible loads. IEEE Trans Autom Sci Eng 2017;14(2):547–57.
[38] Jebamalai JM, Marlein K, Laverge J. Influence of centralized and distributed thermal energy storage on district heating network design. Energy 2020;202:117689.
[39] Li H, Svendsen S, Gudmundsson O, Kuosa M, Rämä M, Sipilä K, et al. Future low temperature district heating design guidebook: final report of IEA DHC annex TS1. IEA; 2017.
[40] Nord N, Shakerin M, Tereshchenko T, Verda V, Borchiellini R. Data informed physical models for district heating grids with distributed heat sources to understand thermal and hydraulic aspects. Energy 2021;222:119965.
[41] Tian Z, Perers B, Furbo S, Fan J. Thermo-economic optimization of a hybrid solar district heating plant with flat plate collectors and parabolic trough collectors in series. Energy Convers Manag 2018;165:92–101.
[42] Shah SK, Aye L, Rismanchi B. Seasonal thermal energy storage system for cold climate zones: a review of recent developments. Renew Sustain Energy Rev 2018;97:38–49.
[43] Köfinger M, Schmidt RR, Basciotti D, Terreros O, Baldvinsson I, Mayrhofer J, et al. Simulation based evaluation of large scale waste heat utilization in urban district heating networks: optimized integration and operation of a seasonal storage. Energy 2018;159:1161–74.
[44] Rohde D, Andresen T, Nord N. Analysis of an integrated heating and cooling system for a building complex with focus on long–term thermal storage. Appl Therm Eng 2018;145:791–803.
[45] Rohde D, Knudsen BR, Andresen T, Nord N. Dynamic optimization of control setpoints for an integrated heating and cooling system with thermal energy storages. Energy 2020;193:116771.
[46] Li H, Hou J, Tian Z, Hong T, Nord N, Rohde D. Optimize heat prosumers' economic performance under current heating price models by using water tank thermal energy storage. Energy 2022;239:122103.
[48] Amrit R, Rawlings JB, Biegler LT. Optimizing process economics online using model predictive control. Comput Chem Eng 2013;58:334–43.
[49] Nocedal J, Wright S. Numerical optimization. Springer Science & Business Media; 2006.
[50] He P, Sun G, Wang F, Wu H, Wu X. Heating engineering (in Chinese). China Architecture & Building Press; 2009.
[51] CEN. CEN/TR16355 Recommendations for prevention of Legionella growth in installations inside buildings conveying water for human consumption. 2012.
[52] Nord, N., Sandberg, N. H., Ngo, H., Nesgård, E., Woszczek, A., Tereshchenko, T., "Future energy pathways for a university campus considering possibilities for energy efficiency improvements." IOP Conference Series: Earth and Environmental Science. 352. 012037. IOP Publishing.
[53] Guan J, Nord N, Chen S. Energy planning of university campus building complex: energy usage and coincidental analysis of individual buildings with a case study. Energy Build 2016;124:99–111.
[54] The modelica Association. https://www.modelica.org/. [Accessed September 2020].
[55] Åkesson J, Gäfvert M, Tummescheit H. Jmodelica- an open source platform for optimization of modelica models.
[56] Tian Z, Zhang S, Deng J, Fan J, Huang J, Kong W, et al. Large-scale solar district heating plants in Danish smart thermal grid: developments and recent trends. Energy Convers Manag 2019;189:67–80.
[57] Larsson O. Pricing models in district heating. 2011.
[58] Charging method for heating bill in Trondheim. https://www.statkraftvarme.no/globalassets/2-statkraft-varme/statkraft-varme-norge/om-statkraft-varme/prisark/20190901/fjernvarmetariff-trondheim-bt1.pdf. [Accessed September 2020].